Canadian Mineralogist
Vol. 20, pp. 349-378 (1982)

LINEAR REGRESSION ANALYSIS OF SILLIMANITE-FORMING REACTIONS AT AZURE LAKE, BRITISH COLUMBIA

LEE C. PIGAGE

Cyprus Anvil Mining Corporation, 300 - 355 Burrard Street, Vancouver, British Columbia V6C 2G8

Abstract

Pelitic metamorphic-mineral assemblages in the Shuswap metamorphic core complex near Azure Lake, British Columbia, are characteristic of the kyanite through sillimanite–muscovite zones of the Barrovian facies-series. Mineral textures delineate a sequence of prograde reactions involving the breakdown of staurolite, garnet and kyanite to form fibrolite–biotite–ilmenite–muscovite aggregrates. Results of microprobe analyses have been combined with linear-regression techniques to outline probable sillimanite-forming reactions. Initial formation of fibrolite has been modeled for the breakdown of staurolite or garnet (or both). The regression equations indicate that rutile is required as a reactant phase. With exhaustion of matrix rutile, garnet becomes a product phase, and continued growth of fibrolite is accompanied by the formation of second-generation garnet. The regression equations all require muscovite as a reactant phase. Textures indicate that muscovite is a late-forming product. These textures probably result from local ionic equilibria and late replacement of fibrolite by muscovite as the K^+/H^+ ratio keeps changing in the fluid phase.

Keywords: Shuswap complex, British Columbia, sillimanite growth, linear regression, garnet and staurolite breakdown.

Sommaire

Les assemblages de minéraux métamorphiques à caractère pélitique dans le noyau métamorphique de Shuswap (près du lac Azure, Colombie-britannique) sont caractéristiques de la zone à disthène jusqu'à la zone à sillimanite + muscovite dans la série de facies barrovienne. Les textures indiquent une série de réactions progrades qui donnent des agrégats de fibrolite + biotite + ilménite + muscovite aux dépens de staurotide, grenat et disthène. Les résultats d'analyses à la microsonde, traités par techniques de régression linéaire, donnent des réactions probablement responsables de la formation de sillimanite. La formation initiale de fibrolite peut s'expliquer par la déstabilisation de staurotide ou grenat (ou des deux). Les équations de régression attribuent au rutile un rôle de réactif; une fois cette phase éliminée, le grenat devient un produit de la réaction. La croissance ininterrompue de la fibrolite est accompagnée par la cristallisation d'un grenat de seconde génération. Toutes les équations de régression nécessitent la muscovite comme réactif; les textures indiquent, cependant, que la muscovite s'est produite tardivement. Ces textures résulteraient d'équilibres ioniques locaux et du remplacement tardif de la fibrolite par la muscovite à mesure que change le rapport K^+/H^+ dans la phase fluide.

(Traduit par la Rédaction)

Mots-clés: complexe de Shuswap, Colombie-britannique, croissance de la sillimanite, régression linéaires, déstabilisation du grenat et de la staurotide.

Introduction

The Shuswap metamorphic core complex in southeastern British Columbia (Fig. 1) is characterized by upper-amphibolite-facies metamorphism and polyphase deformation (Campbell 1977). The northeastern margin of the complex near Azure Lake, British Columbia (Fig. 2) contains the transition from kyanite through sillimanite–muscovite zones of the Barrovian facies-series (Pigage 1978).

Pelites from the Azure Lake area typically contain garnet and staurolite rimmed by aggregates of fibrolite–biotite–muscovite–ilmenite. This study presents the results of a detailed investigation of the sillimanite-forming reactions. Mass-balance calculations using linear regression techniques are combined with results of electron-microprobe analyses to delineate possible metamorphic reactions. Textural relations among the coexisting metamorphic minerals are used to select probable sillimanite-forming reactions from among the different possible mass-balance regression equations.

This report is part of a larger study of deformation and metamorphism on the northeast margin of the Shuswap complex. Briefly, the complex consists of interlayered schist and quartzite units belonging to the Hadrynian Kaza

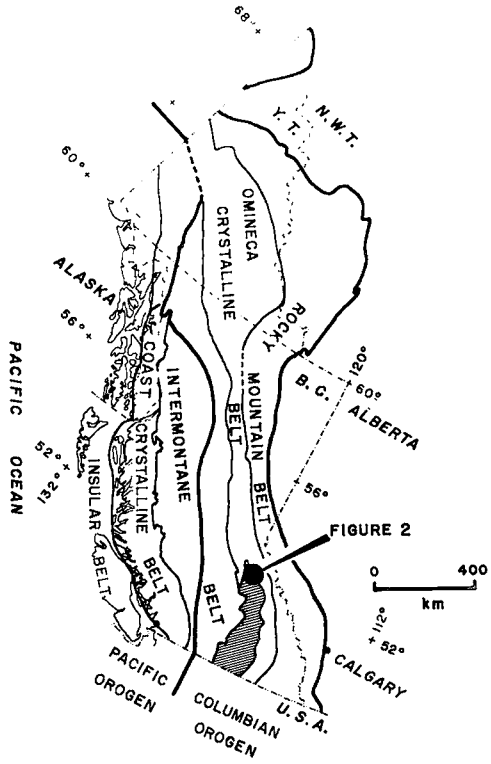

FIG. 1. Major structural elements of the Canadian Cordillera. The Shuswap complex is indicated by the ruled area. The Azure Lake area is indicated (Fig. 2). Modified from Wheeler & Gabrielse (1972).

Group (Sutherland Brown 1963, Campbell 1968). Minor amphibolite and marble units occur throughout the sequence. Two coaxial phases of deformation have been recognized; metamorphism is synchronous with both deformations (Pigage 1978). Comparison of pelite and carbonate metamorphic assemblages with experimental reaction studies results in the following estimate for metamorphic conditions: $T = 605 \pm 50°C$, $P = 5727 \pm 500$ bars, $X(H_2O)$ approximately 0.9 (Pigage & Greenwood, in press; Pigage, in prep.). Deformation and metamorphism were restricted to the time interval between late Triassic and late Jurassic (Pigage 1977).

METHOD OF STUDY

Figure 2 illustrates the locations of 12 pelite samples selected for analysis of major minerals. Estimated modes of these samples are given in Table 1. Analyses (Tables 2–8) were completed using an automated ARL–SEMQ electron microprobe with the following operating conditions: accelerating potential 15 kV, beam diameter 2–35 μm, specimen current 0.02–0.05 μA, counting interval 20 seconds. Beam diameter and specimen current were varied to provide maximum counts with minimum specimen damage. Count readings for a fixed time-interval were normalized to an average beam-current. With fluorine analyses, a counting time of 120 seconds improved the counting statistics.

Analyzed synthetic and natural minerals were used as standards. All readings were corrected for dead time, drift and background. Analytical results for fluorine analyses were computed using a linear regression curve fit to the standards. For all other elements, count readings were corrected for matrix effects using the EMPADR VII program (Rucklidge & Gasparrini 1969).

Several grains of each mineral in a probe mount were analyzed with repeated counts on each grain. All minerals were checked for concentric and sector zoning; where zoning is present (in plagioclase and garnet), the grain edges were considered to represent the composition in equilibrium with the rest of the mineral assemblage. Mean composition and sample variance for each mineral grain were calculated from the results of spot analyses. These mean results were then combined to form an overall mean and standard error for each mineral in a microprobe mount (Bevington 1969).

Iron was computed as FeO. Water content in hydrous minerals was calculated from stoichiometric constraints in the structural formulae. Standard errors for H_2O were computed by a Monte Carlo approach assuming normally distributed random errors in the other analyzed oxides (Anderson 1976).

ASSEMBLAGES OF PELITIC MINERALS

Assemblages of pelitic minerals in the Azure Lake area may be divided into three metamorphic zones (Fig. 2), with metamorphic grade increasing toward the southwest. The assemblages for these zones differ only in the Al_2SiO_5 polymorph present: Al_2SiO_5 (kyanite or sillimanite or both)–garnet–biotite–muscovite–quartz–plagioclase–ilmenite±staurolite (see Table 1). Minor amounts of tourmaline, apatite, zircon, and fine opaque dust (graphite?) are present in each of the assemblages.

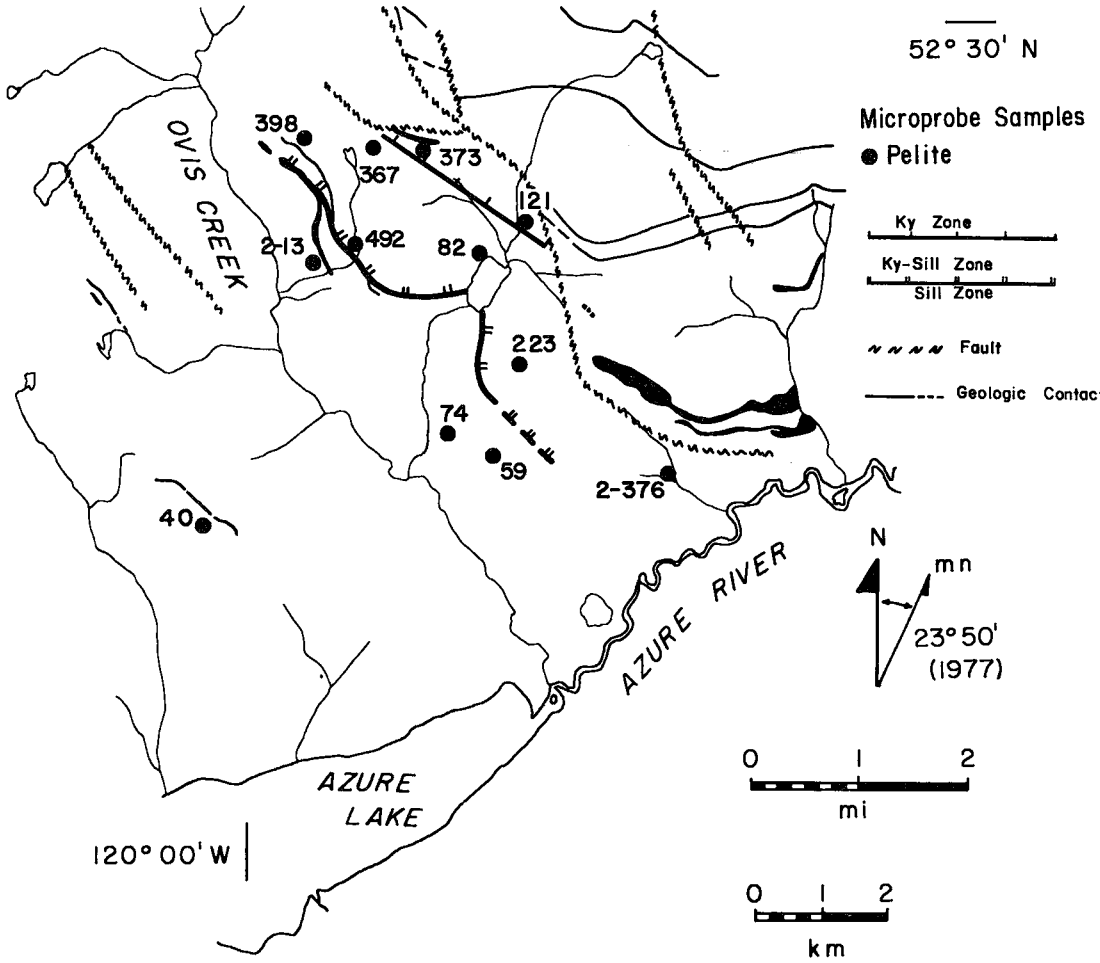

FIG. 2. Metamorphic zones in the Shuswap complex, Azure Lake, British Columbia. Samples selected for electron-microprobe analysis of coexisting minerals are shown. Carbonate units are shown in black.

These assemblages may be described by the ten-component system K_2O–Na_2O–CaO–Al_2O_3–SiO_2–MgO–FeO–MnO–TiO_2–H_2O. Projections for the assemblages are illustrated in Figures 3 to 5. All projections were calculated following the approach outlined by Greenwood (1975). Electron-microprobe results were used to determine the compositions of the different minerals.

The AFM projection (Thompson 1957), with MnO as the fourth corner of a tetrahedron, is used to illustrate phase relations and Mg–Fe–Mn partitioning for coexisting minerals in the different metamorphic zones (Figs. 3A, 4A, 5A). This particular projection assumes that quartz, muscovite, H_2O, ilmenite, albite and anorthite are present in excess or behave as species with fixed chemical potentials.

Garnet is the only mineral that plots away from the AFM plane of the tetrahedron. Tie lines between coexisting minerals are generally subparallel, indicating systematic partitioning of Mg–Fe–Mn between phases. Assemblages in the kyanite and sillimanite zones are at least bivariant in projection. Coexistence of kyanite and sillimanite in the intermediate zone requires univariance if equilibrium was attained.

Figure 6 also illustrates the regular partitioning of Mg–Fe between coexisting garnet and biotite. Partitioning coefficients for each of the

TABLE 1. VISUALLY ESTIMATED MODES FOR MICROPROBE SAMPLES (PERCENT)

SAMPLE	373	121	367	82	398	492	223	2-376	2-13	74	59	40
METAMORPHIC ZONE	K*	K	K-S	K-S	K-S	K-S	K-S	K-S	S	S	S	S
QUARTZ	20	30	2	25	30	20	50	25	30	10	30	25
PLAGIOCLASE	20	17	25	10	15	10	5	15	15	20	15	10
K-FELDSPAR					X#			X	X			
BIOTITE	15	17	35	10	20	15	10	20	15	35	15	14
MUSCOVITE	35	15	30	23	30	35	20	25	35	10	30	25
GARNET	5	10	5	12	3	5	5	5	2	10	6	15
STAUROLITE	2	X		X		2	3					2
KYANITE	3	10	3	15		8	2	7				
SILLIMANITE			X	5	2	5	5	3	3	15	4	7
ILMENITE	X	X	X	X	X	X	X	X	X	X	X	X
RUTILE		IN#		IN		IN	IN					
TOURMALINE	X	X	X	X			X		X	X	X	X
ZIRCON	X	X	X	X	X	X	X	X	X	X	X	X
APATITE	X	X	X					X				X

* K = KYANITE, K-S = KYANITE-SILLIMANITE, S = SILLIMANITE
\# X = PRESENT, IN = INCLUSION

TABLE 2. GARNET ANALYSES

SPECIMEN	373	121	367	82	398	492
ANALYSES	39	11	14	23	14	18
SIO2	37.91(0.05)#	37.05(0.07)	36.51(0.08)	37.74(0.05)	37.37(0.03)	38.05(0.06)
TIO2	-	-	0.02(0.01)	0.01(0.004)	-	0.01(0.003)
AL2O3	20.57(0.03)	21.50(0.04)	21.55(0.04)	21.49(0.03)	21.16(0.06)	21.37(0.02)
FEO*	34.55(0.04)	34.97(0.07)	34.18(0.06)	36.22(0.06)	35.81(0.06)	36.06(0.06)
MNO	1.19(0.01)	1.67(0.04)	1.38(0.05)	1.04(0.02)	2.65(0.03)	1.49(0.06)
MGO	2.75(0.02)	2.87(0.02)	2.90(0.01)	2.81(0.02)	2.76(0.02)	3.01(0.03)
CAO	2.44(0.06)	2.41(0.04)	3.49(0.08)	2.18(0.02)	1.40(0.04)	1.57(0.07)
TOTAL	99.41	100.47	100.03	101.49	101.15	101.56
MOLECULAR PERCENT END-MEMBERS$						
ALMANDINE	78	78	77	80	79	80
SPESSARTINE	3	4	3	2	6	3
PYROPE	11	11	12	11	11	12
GROSSULAR	8	7	9	6	4	5

SPECIMEN	223	2-376	2-13	74	59	40
ANALYSES	16	15	18	14	52	30
SIO2	37.54(0.05)	37.91(0.04)	37.42(0.03)	38.03(0.12)	37.61(0.02)	37.11(0.04)
TIO2	-	0.02(0.004)	-	0.02(0.004)	-	0.01(0.002)
AL2O3	21.17(0.04)	20.84(0.03)	20.58(0.05)	20.82(0.07)	20.56(0.006)	21.53(0.02)
FEO*	35.01(0.05)	35.38(0.04)	34.10(0.05)	33.40(0.10)	34.59(0.02)	36.72(0.05)
MNO	1.46(0.02)	0.75(0.01)	1.69(0.01)	2.37(0.04)	1.27(0.01)	1.04(0.05)
MGO	2.92(0.01)	3.03(0.02)	2.42(0.01)	3.02(0.01)	2.97(0.006)	3.03(0.01)
CAO	2.36(0.03)	2.51(0.04)	2.44(0.02)	2.71(0.02)	2.10(0.01)	1.67(0.03)
TOTAL	100.46	100.44	98.65	100.37	99.10	101.11
MOLECULAR PERCENT END-MEMBERS$						
ALMANDINE	78	79	79	74	78	82
SPESSARTINE	3	2	4	5	3	2
PYROPE	12	12	10	12	12	12
GROSSULAR	7	7	8	8	6	5

\# ESTIMATED STANDARD ERRORS ENCLOSED IN PARENTHESES
* TOTAL IRON AS FEO
$ CALCULATED USING WEIGHTED LINEAR REGRESSION

three metamorphic zones overlap on the diagram; temperature gradients cannot be distinguished.

Figures 3B, 4B and 5B depict phase relations between Al_2SiO_5–muscovite–plagioclase–(K-feldspar) in the subsystem K_2O–Na_2O–CaO–Al_2O_3–SiO_2–H_2O. Tie lines between K-feldspar (samples 2–376, 398, 2–13) and other minerals are dotted because phase relations are problematical.

K-feldspar occurs only as thin selvages (approximately 20 μm thick) partly enclosing some of the plagioclase grains. Results of microprobe analyses show that it is more potassic than muscovite in the same slide (Tables 3, 7). This potassic composition contrasts sharply with K-feldspar compositions reported in studies on the

TABLE 3. MUSCOVITE ANALYSES

SPECIMEN	373	121	367	82	398	492
ANALYSES	20	22	21	13	28	16
SIO2	45.17(0.03)#	46.03(0.06)	46.17(0.13)	46.85(0.08)	45.80(0.05)	47.39(0.09)
TIO2	0.60(0.01)	0.70(0.01)	0.65(0.01)	0.69(0.01)	0.59(0.01)	0.62(0.01)
AL2O3	36.11(0.07)	35.95(0.03)	35.55(0.06)	36.20(0.06)	36.32(0.02)	36.70(0.07)
FEO*	1.02(0.005)	1.18(0.01)	1.13(0.01)	1.21(0.02)	1.06(0.004)	0.99(0.01)
MNO	-	-	-	-	-	-
MGO	0.66(0.006)	0.70(0.01)	0.71(0.02)	0.71(0.01)	0.64(0.01)	0.52(0.01)
CAO	0.01(0.002)	-	-	-	-	0.01(0.004)
BAO	0.26(0.01)	0.35(0.003)	0.27(0.01)	0.41(0.01)	0.34(0.005)	0.50(0.01)
NA2O	1.27(0.006)	1.17(0.01)	1.02(0.01)	1.21(0.02)	1.58(0.02)	1.56(0.03)
K2O	9.18(0.01)	9.40(0.02)	9.77(0.02)	9.42(0.04)	9.11(0.03)	8.59(0.07)
F	0.05(0.003)	0.05(0.001)	0.04(0.002)	0.06(0.003)	0.04(0.002)	0.03(0.002)
H2O$	4.45(0.004)	4.50(0.004)	4.49(0.008)	4.55(0.005)	4.51(0.003)	4.60(0.006)
SUBTOTAL	98.78	100.03	99.80	101.31	99.99	101.51
LESS O=F	0.02	0.02	0.02	0.03	0.02	0.01
TOTAL	98.76	100.01	99.78	101.28	99.97	101.50
MG/(MG+FE)	0.54	0.51	0.53	0.51	0.52	0.48
NA/(NA+K+CA+BA)	0.17	0.16	0.14	0.16	0.21	0.21

SPECIMEN	223	2-376	2-13	74	59	40
ANALYSES	14	31	26	23	19	29
SIO2	45.72(0.09)	45.46(0.04)	46.22(0.08)	44.78(0.07)	45.92(0.05)	46.19(0.03)
TIO2	0.62(0.02)	0.75(0.01)	0.70(0.02)	0.66(0.005)	0.56(0.01)	0.75(0.02)
AL2O3	35.74(0.09)	35.60(0.04)	35.53(0.08)	35.25(0.03)	35.39(0.11)	36.29(0.03)
FEO*	1.10(0.01)	1.18(0.01)	1.29(0.02)	1.91(0.01)	1.20(0.01)	1.11(0.01)
MNO	-	-	0.01(0.002)	0.01(0.003)	-	-
MGO	0.68(0.02)	0.65(0.01)	0.65(0.01)	0.72(0.004)	0.68(0.01)	0.60(0.003)
CAO	0.02(0.004)	-	0.01(0.002)	0.01(0.004)	0.01(0.005)	-
BAO	0.18(0.01)	0.24(0.005)	0.32(0.01)	0.32(0.009)	0.35(0.01)	0.26(0.004)
NA2O	1.17(0.02)	1.11(0.003)	1.02(0.01)	0.89(0.004)	1.14(0.01)	1.32(0.01)
K2O	9.64(0.03)	9.36(0.03)	9.46(0.03)	9.92(0.03)	9.37(0.02)	9.13(0.02)
F	0.06(0.003)	0.04(0.001)	0.05(0.002)	0.07(0.002)	0.04(0.002)	0.07(0.003)
H2O$	4.47(0.007)	4.45(0.003)	4.49(0.006)	4.41(0.004)	4.46(0.007)	4.51(0.003)
SUBTOTAL	99.40	98.84	99.75	98.95	99.12	100.23
LESS O=F	0.03	0.02	0.02	0.03	0.02	0.03
TOTAL	99.37	98.82	99.73	98.92	99.10	100.20
MG/(MG+FE)	0.52	0.50	0.47	0.40	0.50	0.49
NA/(NA+K+CA+BA)	0.15	0.15	0.14	0.12	0.15	0.18

ESTIMATED STANDARD ERRORS ENCLOSED IN PARENTHESES.
* TOTAL IRON AS FEO
$ H2O CALCULATED FROM STRUCTURAL FORMULA (24(O,OH,F)) ASSUMING 4 (OH,F).
STANDARD ERROR FOR H2O CALCULATED FROM STANDARD ERRORS OF OTHER ELEMENTS USING MONTE CARLO APPROACH.

prograde development of K-feldspar by subsolidus reactions or by partial melting (Evans & Guidotti 1966, Lundgren 1966, Guidotti *et al.* 1973, Tracy 1978). In these studies, prograde K-feldspar was found to be consistently more sodic than the coexisting muscovite. Guidotti *et al.* (1973) noted that potassic K-feldspar occurs only in retrograde veinlets transecting the regional K-feldspar + sillimanite assemblages. Because of these considerations, I conclude that the K-feldspar selvages in the Azure Lake area are a retrograde alteration of plagioclase and are not part of the assemblage formed during prograde regional metamorphism.

Figures 3B, 4B, 5B and 7 illustrate the systematic partitioning of Na between plagioclase and muscovite. The diagrams indicate the inverse relationship between anorthite content of plagioclase and paragonite content of coexisting muscovite. Again, the different metamorphic zones do not have distinguishable element partitioning (Fig. 7).

The above compositional relations all support the assumption of chemical near-equilibrium during regional metamorphism. Different projections indicate that the Gibbs phase rule has not been violated. Projections and partitioning diagrams show a systematic partitioning of elements between coexisting minerals. Mineral grains are homogeneous on the scale of a probe section. In contrast, thin selvages of K-feldspar partly enclosing plagioclase probably represent a retrograde alteration of the earlier regional-metamorphic assemblage.

Mineral Textures

Textural relations in the pelite specimens demonstrate that some of the coexisting minerals are not in textural equilibrium. Aggregates of

TABLE 4. BIOTITE ANALYSES

SPECIMEN	373	121	367	82	398	492
ANALYSES	25	25	24	11	24	13
SIO2	35.23(0.07)#	35.65(0.03)	36.73(0.06)	36.81(0.08)	35.71(0.04)	36.27(0.15)
TIO2	1.90(0.01)	2.02(0.02)	1.96(0.02)	2.18(0.02)	1.93(0.01)	2.02(0.02)
AL203	19.14(0.03)	19.48(0.03)	19.59(0.05)	19.50(0.06)	19.24(0.03)	19.39(0.03)
FEO*	19.41(0.04)	18.84(0.02)	18.72(0.01)	19.00(0.04)	19.34(0.02)	18.80(0.03)
MNO	0.02(0.002)	0.03(0.001)	0.02(0.001)	0.01(0.003)	0.06(0.002)	0.02(0.002)
MGO	9.69(0.02)	10.00(0.03)	10.36(0.02)	9.80(0.02)	9.45(0.01)	9.95(0.03)
CAO	0.01(0.002)	-	0.01(0.002)	-	0.01(0.002)	0.01(0.002)
BAO	0.08(0.003)	0.18(0.003)	0.12(0.003)	0.20(0.002)	0.14(0.004)	0.21(0.01)
NA20	0.22(0.002)	0.32(0.003)	0.29(0.01)	0.36(0.01)	0.21(0.003)	0.35(0.01)
K20	8.91(0.03)	8.83(0.02)	9.03(0.03)	8.65(0.05)	9.06(0.01)	8.59(0.01)
F	0.25(0.003)	0.22(0.003)	0.21(0.003)	0.24(0.002)	0.23(0.003)	0.21(0.002)
H20$	3.80(0.005)	3.86(0.003)	3.94(0.005)	3.92(0.005)	3.84(0.003)	3.89(0.008)
SUBTOTAL	98.66	99.43	100.98	100.67	99.22	99.71
LESS O=F	0.11	0.09	0.09	0.10	0.10	0.09
TOTAL	98.55	99.34	100.89	100.57	99.12	99.62
MG/(MG+FE)	0.47	0.49	0.50	0.48	0.47	0.49
NA/2	0.03	0.05	0.04	0.05	0.03	0.05

SPECIMEN	223	2-376	2-13	74	59	40
ANALYSES	22	27	13	18	11	18
SIO2	35.88(0.06)	35.48(0.03)	35.65(0.05)	34.81(0.07)	35.71(0.06)	35.56(0.06)
TIO2	1.76(0.02)	2.23(0.02)	2.15(0.003)	2.52(0.005)	2.30(0.02)	2.06(0.02)
AL203	19.43(0.04)	19.11(0.03)	19.00(0.01)	18.80(0.02)	19.22(0.03)	19.40(0.03)
FEO*	18.68(0.04)	18.72(0.03)	19.45(0.02)	18.99(0.04)	18.54(0.07)	18.88(0.07)
MNO	0.02(0.002)	0.01(0.002)	0.03(0.003)	0.04(0.002)	0.02(0.004)	0.01(0.002)
MGO	10.22(0.03)	9.75(0.02)	9.26(0.02)	9.76(0.01)	9.63(0.02)	9.89(0.05)
CAO	0.01(0.001)	0.01(0.002)	0.02(0.002)	-	0.02(0.002)	-
BAO	0.09(0.004)	0.11(0.002)	0.19(0.003)	0.15(0.005)	0.14(0.01)	0.14(0.01)
NA20	0.32(0.003)	0.28(0.003)	0.31(0.01)	0.26(0.003)	0.36(0.004)	0.35(0.01)
K20	8.73(0.01)	8.82(0.03)	8.76(0.03)	9.13(0.01)	8.65(0.03)	8.30(0.03)
F	0.32(0.003)	0.27(0.002)	0.27(0.002)	0.24(0.003)	0.21(0.003)	0.32(0.009)
H20$	3.82(0.004)	3.80(0.003)	3.80(0.004)	3.79(0.004)	3.84(0.005)	3.79(0.006)
SUBTOTAL	99.28	98.59	98.89	98.49	98.64	98.70
LESS O=F	0.13	0.11	0.11	0.10	0.09	0.13
TOTAL	99.15	98.48	98.78	98.39	98.55	98.57
MG/(MG+FE)	0.49	0.48	0.46	0.48	0.50	0.48
NA/2	0.05	0.04	0.05	0.04	0.05	0.05

ESTIMATED STANDARD ERRORS ENCLOSED IN PARENTHESES
* TOTAL IRON AS FEO
$ H20 CALCULATED FROM STRUCTURAL FORMULA (24(O,OH,F)) ASSUMING 4 (OH,F).
STANDARD ERROR FOR H20 CALCULATED FROM STANDARD ERRORS OF OTHER ELEMENTS USING MONTE CARLO APPROACH.

TABLE 5. STAUROLITE ANALYSES

SPECIMEN	373	82	492	223	40
ANALYSES	66	6	21	12	43
SIO2	28.24(0.04)#	27.40(0.09)	28.10(0.09)	27.60(0.05)	27.33(0.03)
TIO2	0.59(0.003)	0.68(0.05)	0.63(0.01)	0.71(0.005)	0.53(0.01)
AL203	54.51(0.03)	53.67(0.21)	54.58(0.11)	53.90(0.05)	54.59(0.08)
FEO*	11.67(0.02)	13.30(0.05)	13.59(0.07)	13.76(0.02)	13.34(0.04)
ZNO	0.84(0.004)	1.18(0.03)	0.90(0.01)	0.71(0.005)	1.32(0.01)
MNO	0.01(0.005)	0.05(0.004)	0.06(0.002)	0.07(0.002)	0.04(0.002)
MGO	1.16(0.01)	1.43(0.06)	1.75(0.03)	1.59(0.02)	1.50(0.01)
CAO	-	0.01(0.004)	-	-	-
F	NA	-	-	0.01(0.002)	0.01(0.002)
H20$	2.16(0.001)	2.15(0.007)	2.19(0.007)	2.15(0.002)	2.16(0.002)
TOTAL	99.18	99.87	101.80	100.51	100.82
MG/(MG+FE)	0.15	0.16	0.19	0.17	0.17

ESTIMATED STANDARD ERRORS ENCLOSED IN PARENTHESES
* TOTAL IRON AS FEO
NA = NOT ANALYZED
$ H20 CALCULATED FROM STRUCTURAL FORMULA (48 (O,OH,F)) ASSUMING 4 (OH,F).
STANDARD ERROR FOR H20 CALCULATED FROM STANDARD ERRORS OF OTHER ELEMENTS USING MONTE CARLO APPROACH.

TABLE 6. PLAGIOCLASE ANALYSES

SPECIMEN	373	121	367	82	398	492
ANALYSES	32	36	25	23	28	19
SIO2	61.22(0.18)#	60.60(0.19)	58.19(0.13)	61.60(0.07)	63.54(0.07)	63.96(0.17)
AL203	24.25(0.12)	26.30(0.10)	26.35(0.08)	23.98(0.04)	22.73(0.04)	23.49(0.04)
CAO	5.74(0.12)	6.41(0.11)	8.09(0.04)	5.94(0.04)	4.39(0.03)	4.74(0.03)
NA20	8.19(0.08)	7.69(0.04)	6.84(0.03)	8.46(0.03)	9.19(0.03)	8.75(0.03)
K20	0.07(0.004)	0.07(0.002)	0.06(0.002)	0.07(0.003)	0.08(0.004)	0.05(0.002)
BAO	0.02(0.004)	0.01(0.003)	0.01(0.002)	-	0.01(0.003)	0.01(0.003)
TOTAL	99.49	101.08	99.54	100.05	99.94	101.00
MOLECULAR PERCENT END-MEMBERS$						
ANORTHITE	27.7	33.8	39.2	26.8	20.0	22.5
ALBITE	71.9	66.1	60.2	72.6	79.4	76.0
ORTHOCLASE	0.4	0.4	0.3	0.4	0.5	0.3
RANGE (AN)	20-33	23-35	35-41	21-30	20-25	17-25
ZONING	REVERSE	REVERSE	-	REVERSE	-	REVERSE

SPECIMEN	223	2-376	2-13	74	59	40
ANALYSES	12	19	31	10	33	22
SIO2	59.37(0.11	61.24(0.11)	60.24(0.10)	60.37(0.18)	60.98(0.10)	62.90(0.07)
AL203	25.03(0.07	24.31(0.04)	24.76(0.05)	25.13(0.08)	24.10(0.02)	23.67(0.03)
CAO	7.18(0.11)	5.74(0.06)	6.50(0.04)	7.31(0.07)	5.33(0.03)	5.08(0.02)
NA20	7.71(0.05)	8.16(0.03)	7.91(0.03)	7.20(0.17)	8.46(0.02)	8.88(0.003)
K20	0.07(0.003)	0.08(0.003)	0.09(0.006)	0.05(0.005)	0.09(0.003)	0.06(0.003)
BAO	0.02(0.004)	-	-	-	-	0.01(0.002)
TOTAL	99.38	99.53	99.50	100.06	98.96	100.60
MOLECULAR PERCENT END-MEMBERS$						
ANORTHITE	32.9	27.9	30.9	33.5	26.4	23.7
ALBITE	66.5	71.4	68.6	66.0	73.6	75.8
ORTHOCLASE	0.4	0.5	0.5	0.3	0 5	0.3
RANGE (AN)	33-38	22-29	26-34	33-38	24-30	23-26
ZONING	-	REVERSE	REVERSE	-	-	-

ESTIMATED STANDARD ERRORS ENCLOSED IN PARENTHESES
$ CALCULATED USING WEIGHTED LINEAR REGRESSION

TABLE 7. K-FELDSPAR ANALYSES

SPECIMEN	398	2-376	2-13
ANALYSES	2	7	5
SIO2	64.46(1.39)#	64.81(0.24)	64.50(0.34)
AL203	19.24(0.26)	18.22(0.07)	17.75(0.07)
CAO	0.02(0.00)	0.01(0.004)	0.13(0.09)
NA20	0.22(0.03)	0.20(0.009)	0.18(0.004)
K20	15.04(0.68)	15.74(0.16)	15.51(0.14)
BAO	0.31(0.02)	0.25(0.005)	0.50(0.01)
TOTAL	98.85	99.75	99.29
MOLECULAR PERCENT END-MEMBERS$			
ANORTHITE	0.1	-	0.7
ALBITE	2.2	1.9	1.7
ORTHOCLASE	97.0	97.6	96.7
CELSIAN	0.7	0.5	0.9

ESTIMATED STANDARD ERRORS ENCLOSED IN PARENTHESES
$ CALCULATED USING WEIGHTED LINEAR REGRESSION

fibrolitic sillimanite–ilmenite–biotite–muscovite appear to have formed at the expense of garnet, staurolite and kyanite. These textures outline a sequence of reactions that have been partially preserved by growth patterns in various minerals. In the following sections the textures are described and related to possible metamorphic reactions.

Garnet porphyroblasts in all three metamorphic zones outline two stages of growth (Figs. 8, 9B). First-stage garnet forms large, ragged grains with abundant inclusions of quartz, pla-

TABLE 8. ILMENITE ANALYSES

SPECIMEN	373	121	367	82	398	492
ANALYSES	5	9	11	6	8	11
TIO2	51.77(0.08)#	51.66(0.17)	52.52(0.21)	52.76(0.11)	53.22(0.25)	52.76(0.11)
AL203	0.15(0.11)	0.01(0.007)	0.02(0.006)	0.06(0.008)	0.06(0.05)	0.15(0.11)
FEO*	45.33(0.12)	44.29(0.12)	46.90(0.08)	46.67(0.09)	45.21(0.22)	46.45(0.17)
ZNO	NA	0.03(0.003)	0.03(0.006)	0.04(0.007)	0.04(0.007)	0.06(0.006)
MNO	0.85(0.01)	0.39(0.01)	0.51(0.02)	0.25(0.01)	1.38(0.03)	0.33(0.02)
MGO	0.06(0.002)	0.04(0.01)	0.05(0.003)	0.07(0.02)	0.03(0.004)	0.10(0.04)
CAO	-	0.09(0.02)	0.02(0.01)	-	0.01(0.004)	-
TOTAL	98.16	96.51	100.05	99.85	99.95	99.64

SPECIMEN	223	2-376	2-13	74	59	40
ANALYSES	11	9	9	1	5	8
TIO2	52.22(0.11)	52.29(0.21)	51.23(0.12)	49.62	52.73(0.06)	52.84(0.20)
AL203	0.02(0.003)	0.17(0.14)	0.02(0.01)	0.02	0.04(0.002)	0.02(0.004)
FEO*	46.45(0.17)	46.07(0.27)	44.29(0.16)	44.99	44.13(0.09)	46.87(0.10)
ZNO	0.03(0.006)	0.06(0.007)	0.15(0.06)	0.06	0.06(0.009)	0.06(0.005)
MNO	0.31(0.006)	0.27(0.02)	0.76(0.03)	1.78	1.18(0.009)	0.18(0.004)
MGO	0.14(0.02)	0.03(0.003)	0.03(0.01)	0.02	0.03(0.004)	0.32(0.02)
CAO	-	0.01(0.003)	0.05(0.02)	--	0.01(0.004)	-
TOTAL	99.17	98.90	96.53	96.70	98.18	100.29

NA = NOT ANALYZED
# ESTIMATED STANDARD ERRORS ENCLOSED IN PARENTHESES
* TOTAL IRON AS FEO

gioclase, mica and opaque minerals. Typically they contain an even, sparse, opaque dusting. Individual porphyroblasts are partly to completely enclosed by aggregates of intergrown fibrolite, coarse muscovite, xenoblastic ilmenite and biotite (Figs. 9, 11). Breakdown of garnet to form these aggregates is more extensive with increasing metamorphic grade. First-stage garnet is commonly not preserved southwest of Ovis Creek (Fig. 2). Staurolite and kyanite porphyroblasts form similar relict grains within aggregates of muscovite or fibrolite–muscovite. Fibrolite coarsens to form sillimanite prisms with increasing metamorphic grade.

Second-stage garnet forms clear, idioblastic rims around ragged, first-stage garnet cores. These rims contain only minor inclusions (Figs. 8, 9B). Where first-stage garnet is uncommon, second-generation garnet forms small idioblastic porphyroblasts. Fibrolite, biotite and ilmenite are partly to completely enclosed by second-stage rims (Figs. 8, 11). Growth of second-stage garnet succeeded initial formation of the fibrolite aggregates.

Chemical zoning patterns in garnet also reflect two stages of growth. Traverses across selected garnet grains are shown in Figure 8. First-stage-garnet cores are compositionally homogeneous. Second-generation rims are concentrically zoned, with spessartine content decreasing outward. Almandine content varies inversely with spessartine. In most samples, pyrope and grossular contents remain fairly constant. In sample 367 grossular and pyrope concentrations are also concentrically zoned. Zoning patterns in small grains of second-stage garnet at higher metamorphic grades (sample 40, Fig. 8D) are similar but are limited in range.

This zoning is similar to the "normal" zoning pattern described for metamorphic garnet from pelitic schist (Harte & Henley 1966, among others). Hollister (1966) suggested a fractionation – depletion model to explain the distinctive concentric Mn-zoning. Recently, it has been suggested that the zoning results from continuous garnet-forming reactions during prograde metamorphism (Tracy *et al.* 1976, Trzcienski 1977). In kyanite- and sillimanite-bearing schists, diffusion assumes increased importance in modifying the original pattern of growth zoning (Anderson & Olimpio 1977, Woodsworth 1977). Thompson *et al.* (1977) have further argued that internal chemical and inclusion discontinuities in garnet from Vermont resulted from resorption of garnet through a discontinuous reaction involving garnet as a reactant phase.

The sharp change in inclusion density between stage-one and stage-two garnets from the Azure Lake area suggests that each generation of growth was formed through a separate metamorphic reaction. Stage-one garnet probably formed through a continuous, prograde, garnet-forming reaction during low- to medium-amphibolite-facies metamorphism. These stage-one garnets were then partially to completely resorbed through a metamorphic reaction involving the formation of fibrolite aggregates. The pattern of chemical zoning in first-generation

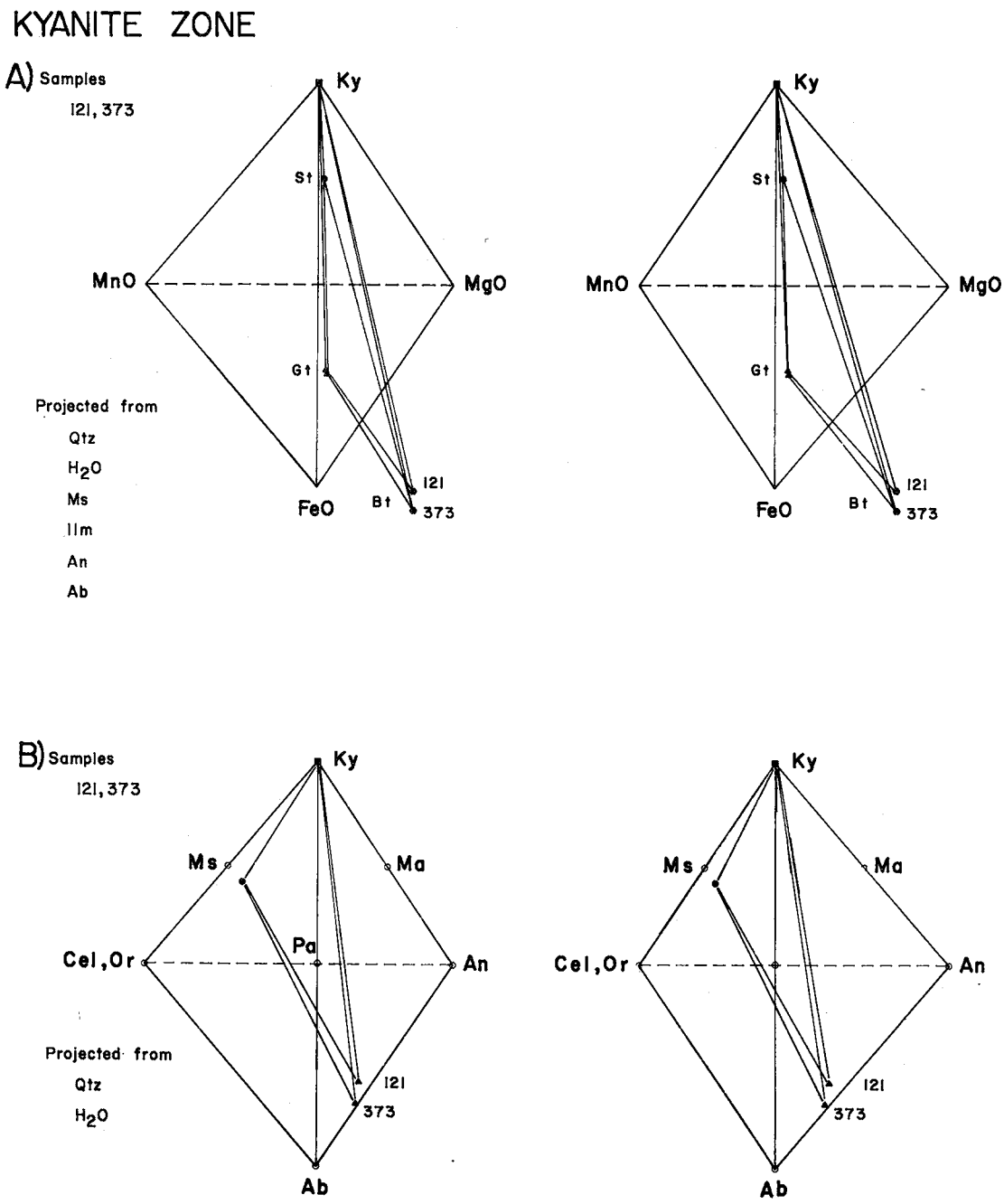

FIG. 3. Stereoscopic projections of analyzed pelitic assemblages in the kyanite zone. A) Modified AFM projection with MnO as the fourth corner of the tetrahedron. B) Projected phase relations in the subsystem K_2O–Na_2O–CaO–Al_2O_3–SiO_2–H_2O. Abbreviations: Ab albite, An anorthite, Bt biotite, Cel celadonite, Ilm ilmenite, Gt garnet, Ky kyanite, Ma margarite, Ms muscovite, Or orthoclase, Pa paragonite, Sil sillimanite, St staurolite.

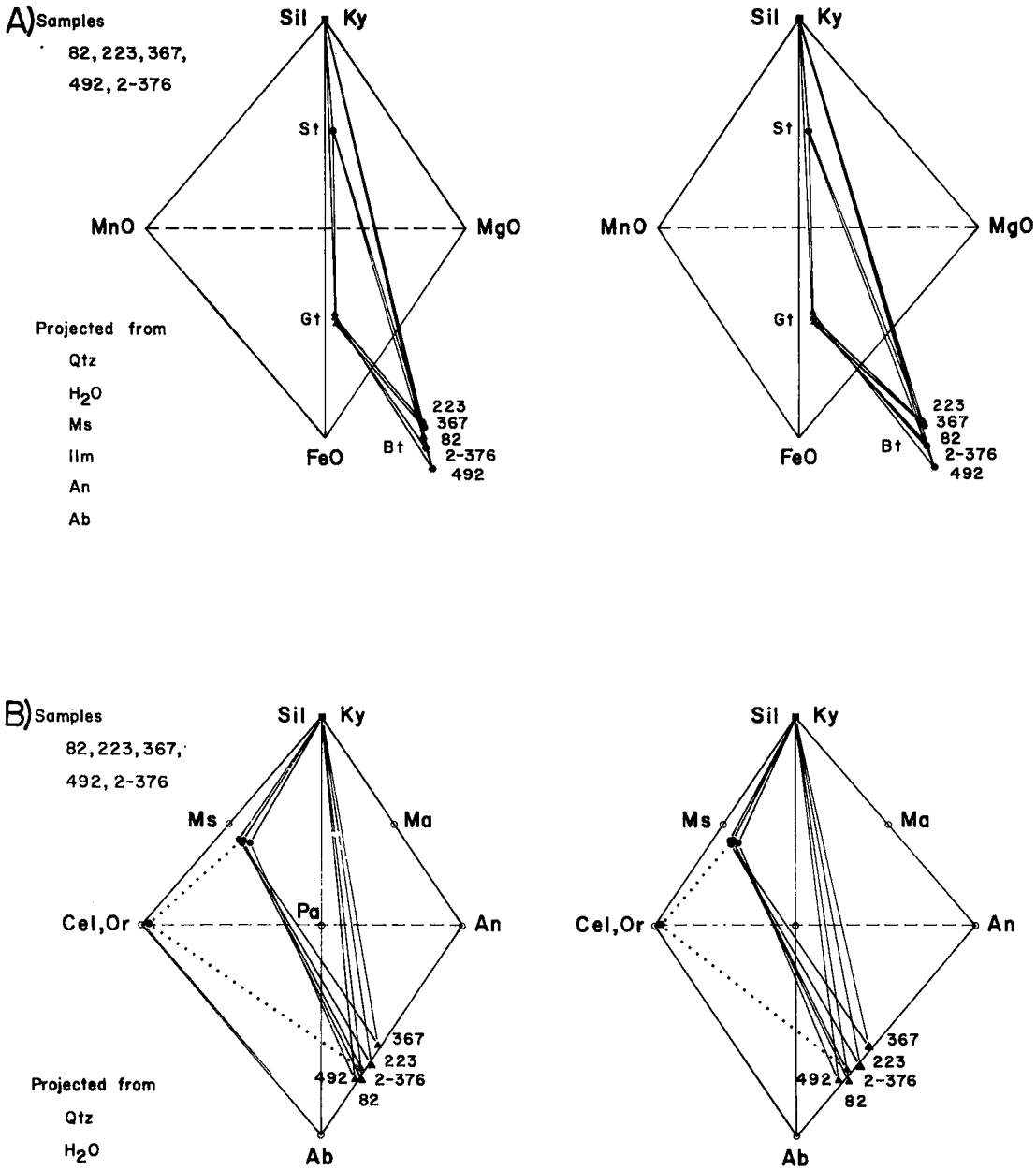

FIG. 4. Stereoscopic projections of analyzed pelitic assemblages in the kyanite–sillimanite zone. A), B) and abbreviations are the same as in Fig. 3.

garnet is compatible with homogenization by diffusion in the garnet concomitant with the formation of the fibrolite aggregates. Concentric zoning in second-generation garnet resulted from subsequent growth according to a continuous garnet-forming reaction during prograde meta-

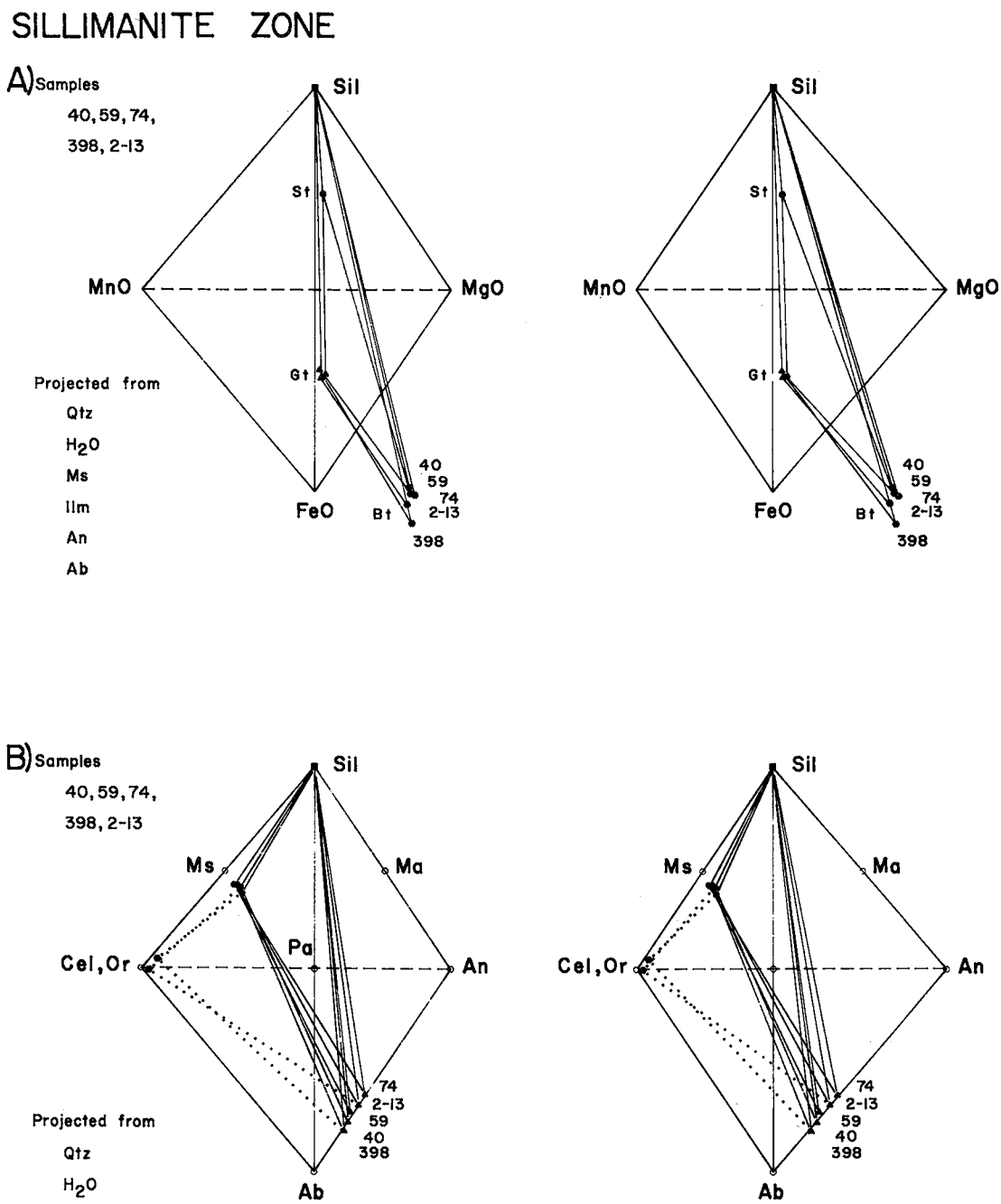

FIG. 5. Stereoscopic projections of analyzed pelitic assemblages in the sillimanite zone. A), B) and abbreviations are the same as in Fig. 3.

morphism. This suggested sequence of reactions may be due to a single prograde metamorphic episode.

Muscovite in the fibrolite aggregates typically forms coarse, equant, randomly oriented flakes. Individual grains are interlocking with

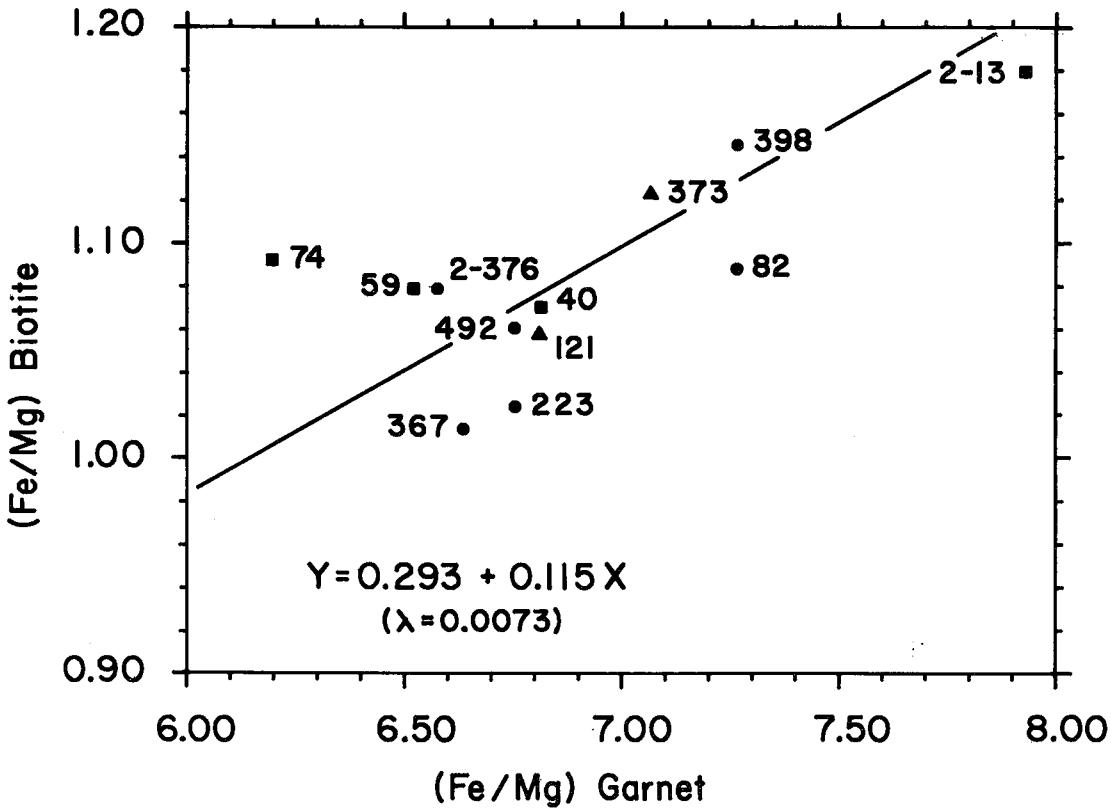

FIG. 6. Fe–Mg distribution between garnet and biotite rim compositions. "Best fit" linear equation was calculated recognizing that both variables are subject to error (Mark & Church 1977). Value for λ: (sample variance of y) / (sample variance of x); triangle kyanite zone, circle kyanite–silimanite zone, square sillimanite zone.

ragged margins (Figs. 9, 10, 11, 12). Fibrolite content in aggregates varies inversely with the modal amount of muscovite; aggregates in quartzitic pelite units commonly contain mainly muscovite. At higher metamorphic grades biotite–fibrolite aggregates form attenuated trails through coarse muscovite grains (Fig. 12).

Plagioclase commonly forms elongate augen conformable with the regional schistosity. Grains are rarely twinned. In many instances, grains are concentrically zoned with a narrow rim of more calcic composition. Since plagioclase is the only major Ca-bearing phase besides garnet in the pelite specimens, zoning is probably related to garnet breakdown.

These textures describe the initial breakdown of garnet, staurolite and kyanite to form aggregates of fibrolite–muscovite–biotite–ilmenite. Growth of second-stage garnet occurred after the initial formation of the fibrolite aggregates. Replacement textures within aggregates at higher metamorphic grades also imply that muscovite growth continued beyond formation of the fibrolite.

METAMORPHIC REACTIONS

Described textural relations support the following sillimanite-forming reactions (all unbalanced) in the system K_2O–FeO–MgO–Al_2O_3–SiO_2–H_2O (KFMASH) (Thompson 1976):

Garnet + Muscovite = Sillimanite + Biotite + Quartz (1)
(Stage-one garnet breakdown)

Staurolite + Muscovite + Quartz = Sillimanite + Biotite + H_2O (2)

Kyanite = Sillimanite (3)

Staurolite + Quartz = Sillimanite + Garnet + H_2O (4)
(Stage-two garnet growth)

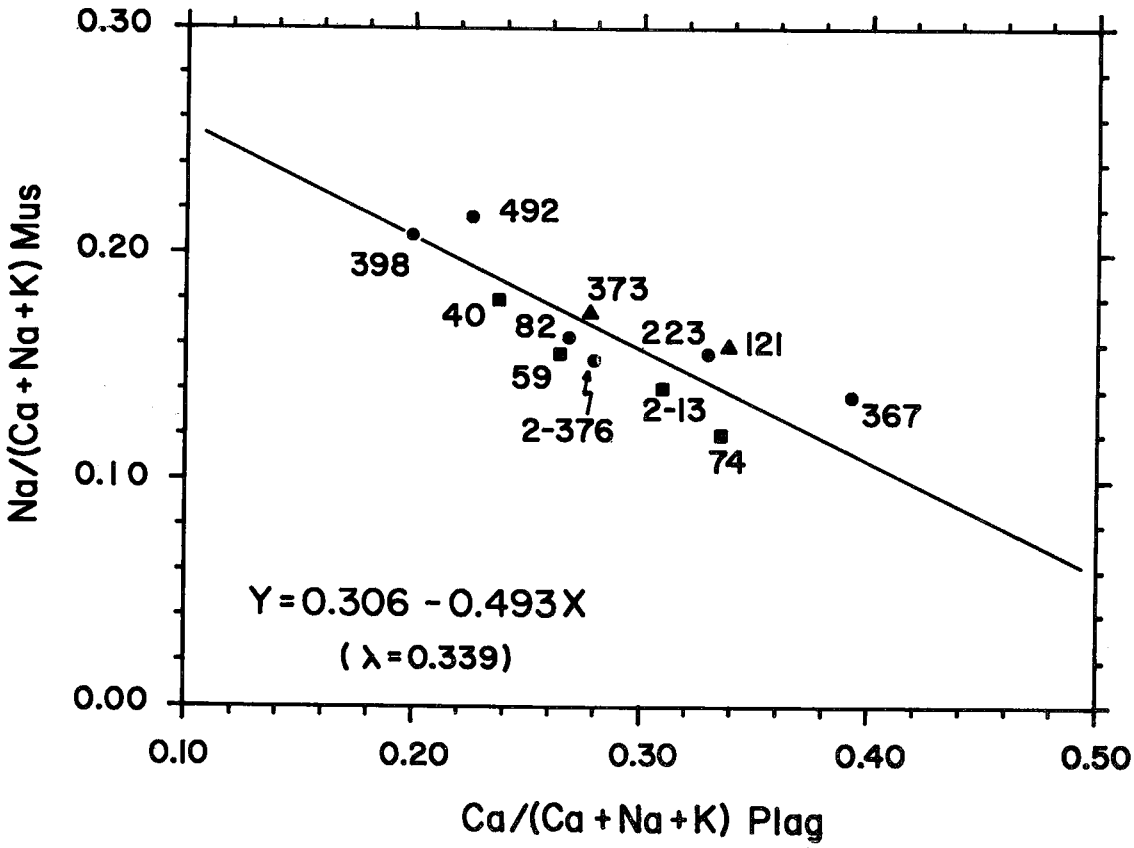

FIG. 7. Na–Ca distribution between plagioclase and muscovite rim compositions. "Best fit" linear equation was calculated recognizing that both variables are subject to error (Mark & Church 1977). Value for λ: variance of y / (variance of x); triangle kyanite zone, circle kyanite–sillimanite zone, square sillimanite zone.

Reactions (1), (2) and (4) are continuous in the system KFMASH; they occur over an isobaric temperature interval because of Mg–Fe partioning. These reactions do not account for grossular content in garnet, paragonite content in muscovite, or Ti content in biotite. Additional phases needed to incorporate these elements are plagioclase and ilmenite.

Muscovite is required as a reactant phase in reactions (1) and (2). Textures indicate that coarse muscovite is a product phase within the fibrolite aggregates and is replacing kyanite and staurolite. This apparent discrepancy may be explained by local cation-exchange reactions or changes in composition of the fluid phase (or both). Both possibilities are discussed later.

Similar sillimanite-forming reactions have been described from other regionally metamorphosed terranes (Chakraborty & Sen 1967, Yardley 1977). Textural descriptions for garnet breakdown in pelite from Connemara, Ireland are especially comparable (Yardley 1977). Reactions (1) and (2) contrast with the commonly observed reaction involving the breakdown of staurolite and muscovite to form garnet, biotite and sillimanite (Thompson 1976, Carmichael 1970).

LINEAR REGRESSION

The use of linear regression techniques to solve the mass-balance constraints implied by possible metamorphic reactions has been previously outlined (Greenwood 1968, Reid *et al.* 1973, Gray 1973, Pigage 1976). Briefly, the method uses a least-squares approach to test for linear dependencies among sets of minerals (vectors) in one or more assemblages. Textural relations are needed to select probable reactions from among the different possible mass-balance

regression-equations. This approach necessarily assumes that metamorphic reactions are isochemical.

A particular mass-balance equation is considered significant if the residual difference between the observed and modeled compositions is smaller than the combined estimates of precision for the mineral and the model. In an earlier

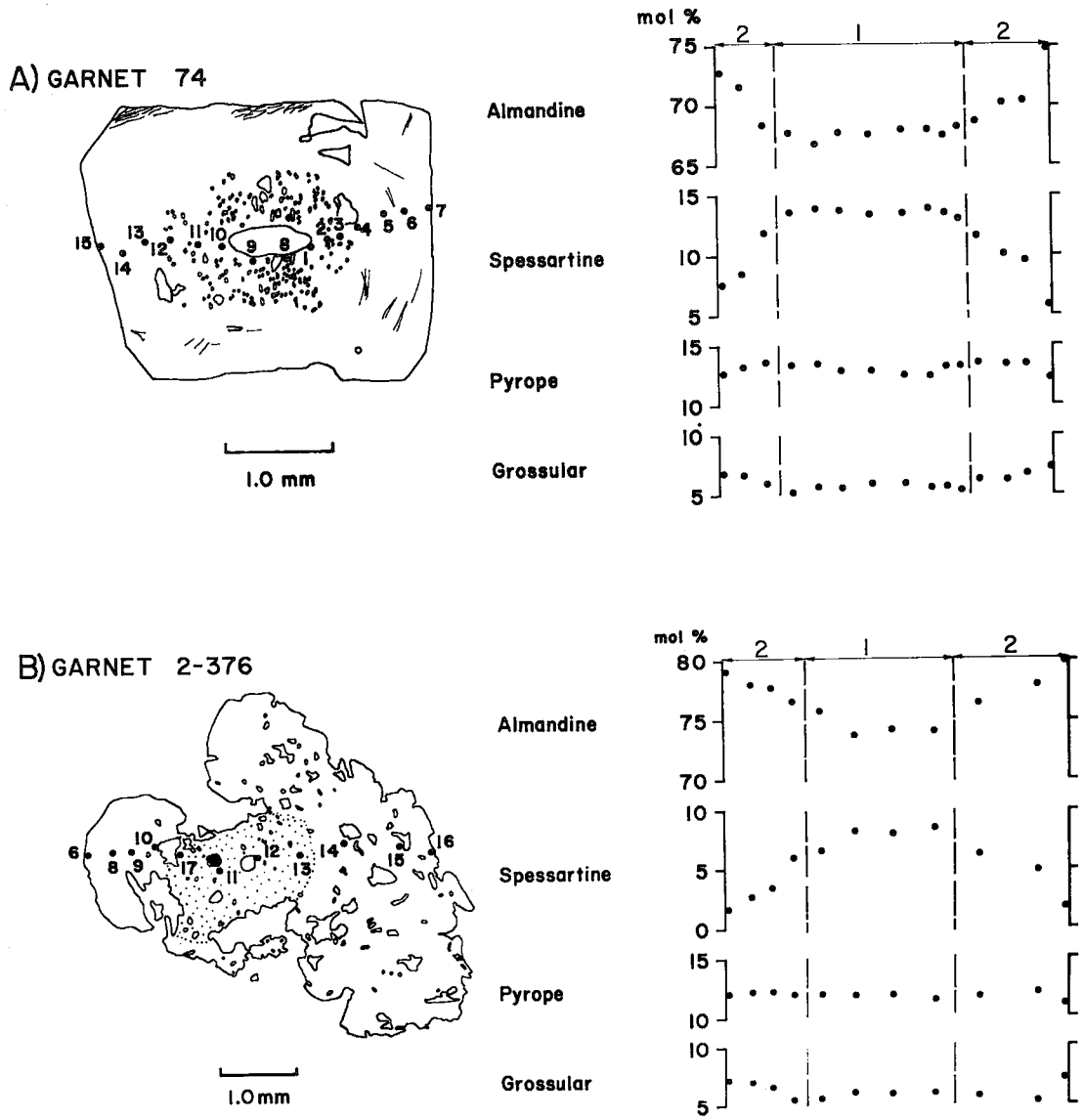

FIG. 8. Patterns of chemical zoning in selected grains of garnet. Spot analyses were obtained with the electron microprobe. Brief descriptions of the grains are given below: A) Sample 74. First-generation garnet with numerous inclusions enclosed by a rim containing fibrolite inclusions. B) Sample 2-376. Small first-generation-garnet core containing opaque dust surrounded by large second-generation-garnet

C) GARNET 367

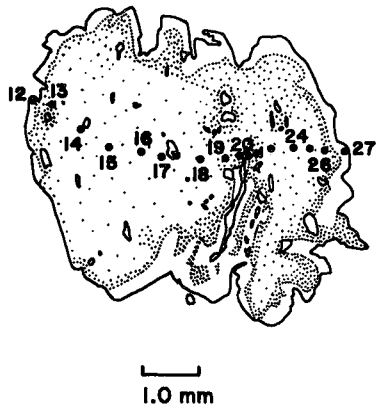

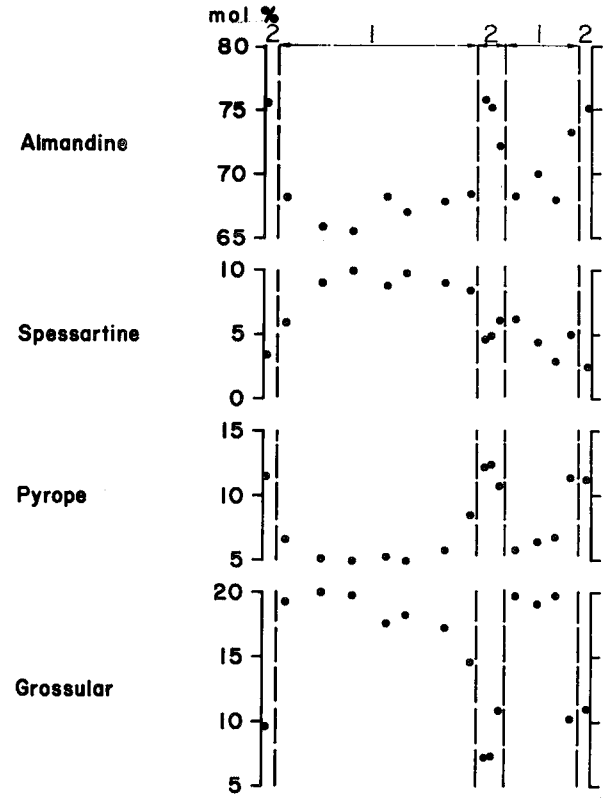

D) GARNET 40

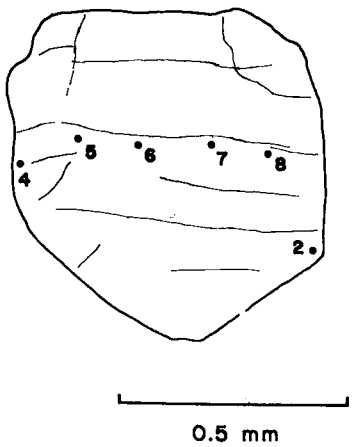

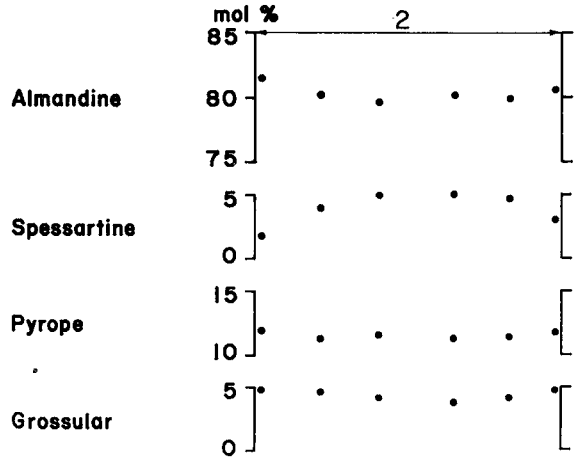

rim. C) Sample 367. Large first-generation garnet with narrow second-generation rim. Chemical zoning involves grossular and pyrope as well as almandine and spessartine. Zoning anomaly for analyses 20 and 21 is stage-two garnet growing in deep embayment in stage-one garnet. D) Sample 40. Small second-generation garnet from southwest of Ovis Creek.

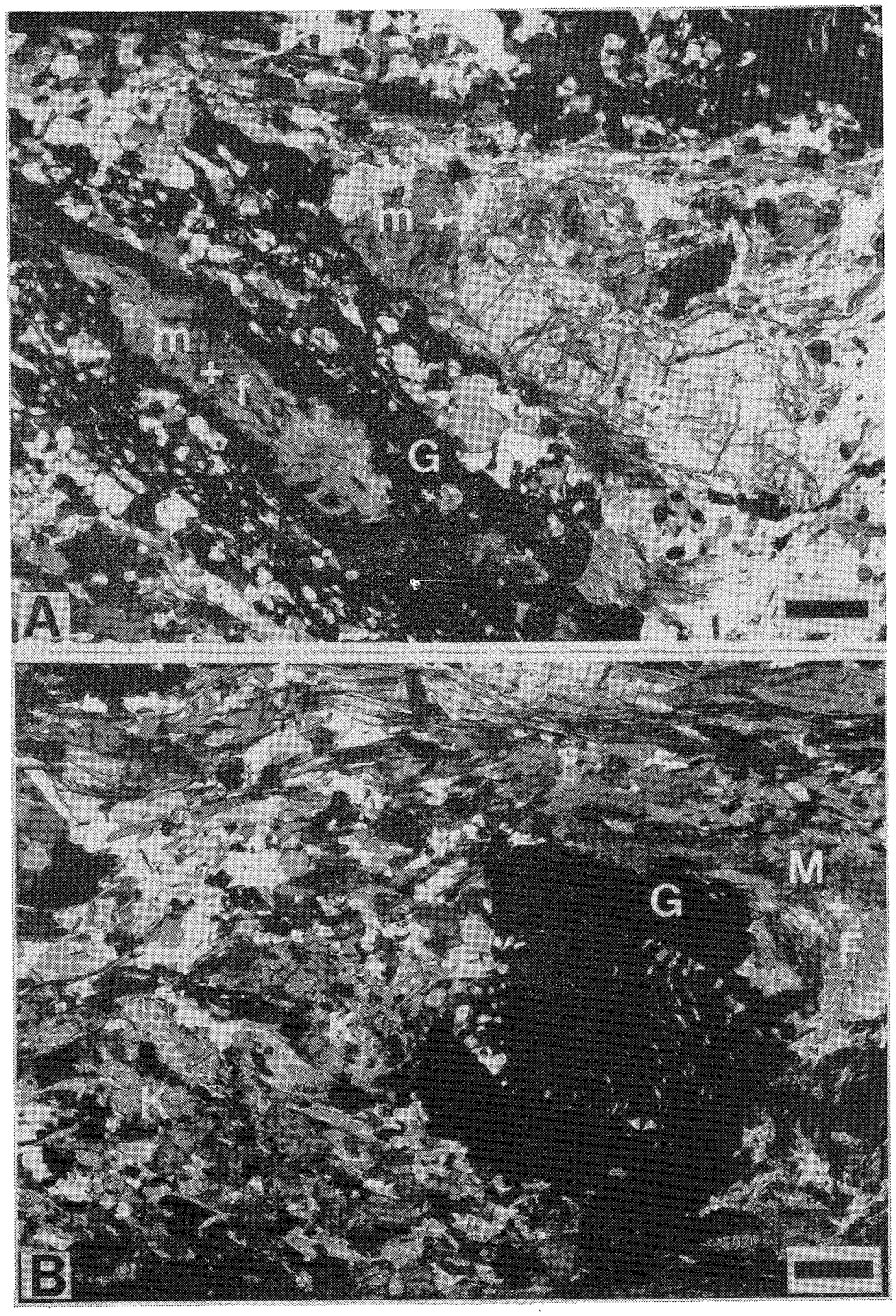

FIG. 9 A.) Schist from the sillimanite zone, Shuswap complex. Staurolite(s) and garnet(G) are surrounded by equant, porphyroblastic muscovite with fibrolite (m + f). Inclusion trails in garnet are straight. Scale bar is 1 mm; crossed nicols. B) Schist from the kyanite–sillimanite zone, Shuswap complex. First-stage garnet contains S-shaped inclusions trails. Second-stage-garnet rim (outer margin) contains only a few scattered inclusions. Garnet is partly surrounded by porphyroblastic muscovite–fibrolite aggregate(M + F). Kyanite(K) is common in the schist's matrix. Scale bar is 1 mm; crossed nicols.

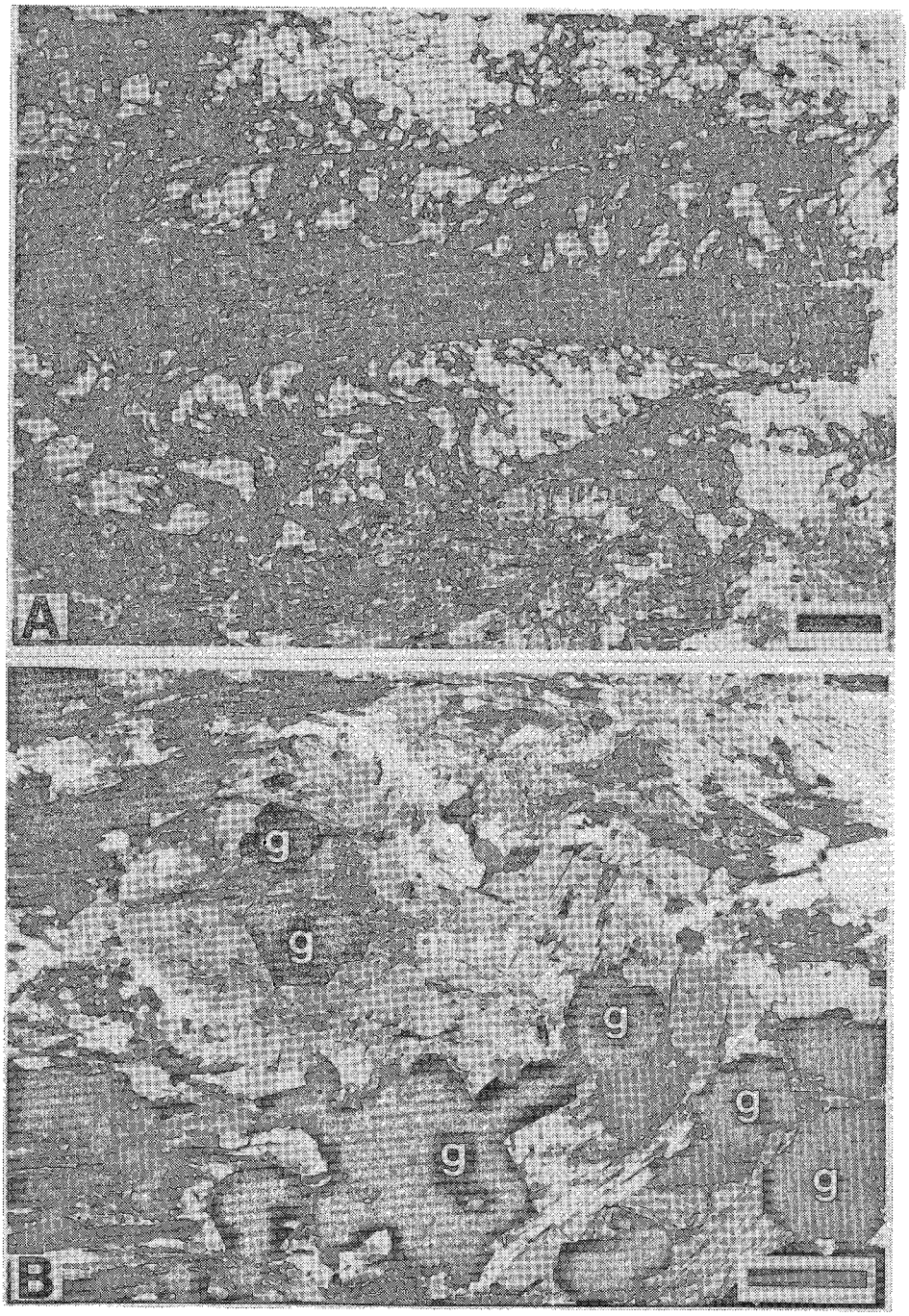

FIG. 10. A) Schist from the kyanite–sillimanite zone, Shuswap complex. Quartz inclusions outline a relict crenulation cleavage in this large stage-one garnet. Opaque inclusions are continuous with the external P1 schistosity, although rotated relative to it. Fibrolite aggregates occur in the lower portion of the photomicrograph. Scale bar is 1 mm; plane light. B) Schist from the sillimanite zone, Shuswap complex. Idioblastic grains of second-stage garnet(g) are enclosed by porphyroblastic muscovite with minor fibrolite(m + f). The large muscovite grains have a random orientation and interlocking grain margins. Scale bar is 1 mm; crossed nicols.

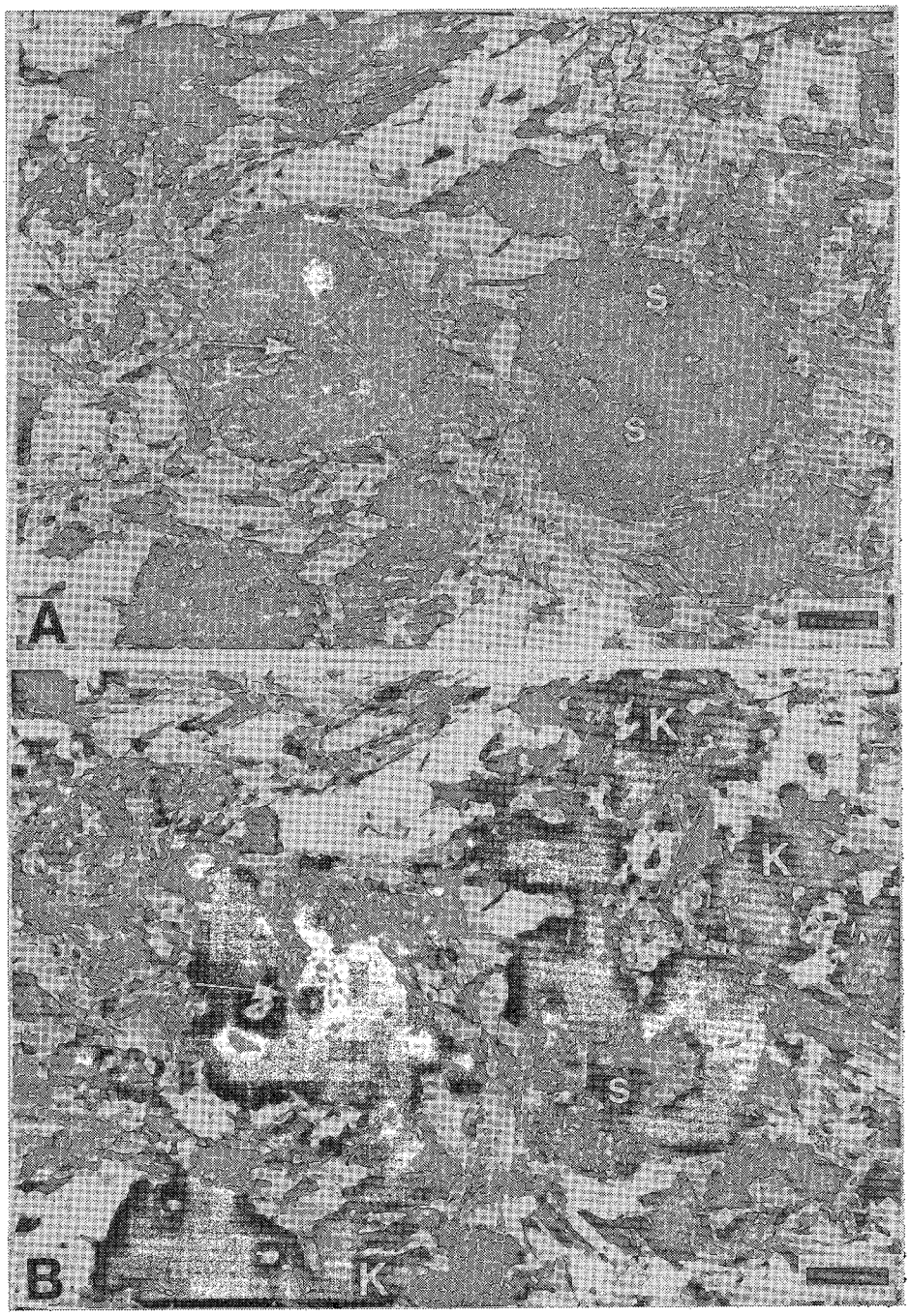

FIG. 11. Schist from the kyanite–sillimanite zone, Shuswap complex. Garnet and staurolite(s) are partly enclosed by fibrolite–muscovite–ilmenite aggregates. Kyanite(k) is abundant in the schist matrix. Arrow points to area where fibrolite is partly enclosed by second-stage garnet. Second-stage-garnet rims are euhedral against the fibrolite aggregates. Scale bar is 1 mm. A) plane light; B) crossed nicols.

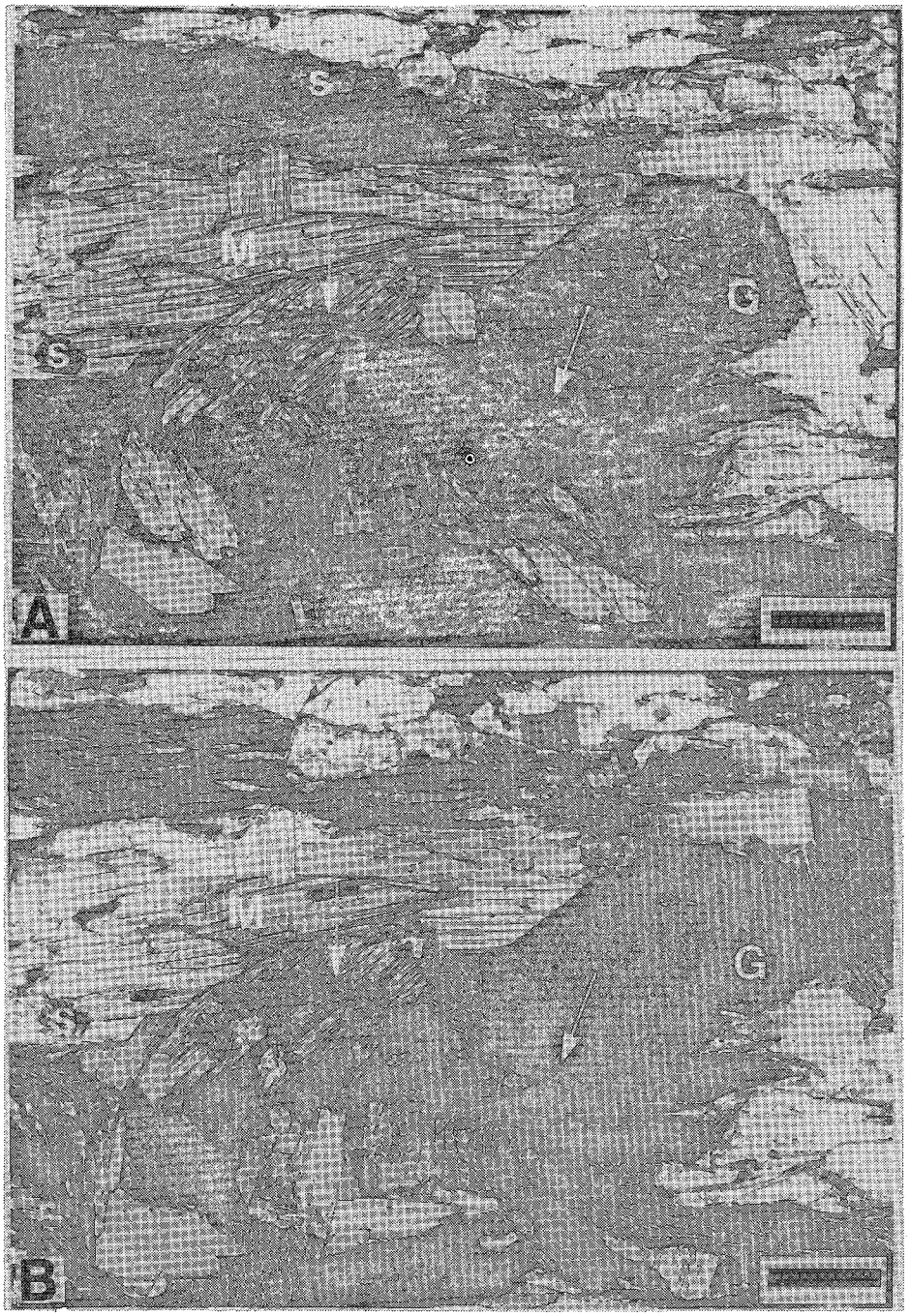

FIG. 12. Schist from the sillimanite zone, Shuswap complex. Porphyroblastic muscovite(m) is randomly oriented in the schist matrix. Fibrolite–biotite aggregates form attenuated wispy trails through the muscovite (arrows). Relict staurolite(s) is enclosed by fibrolite or muscovite. Arrow in second-generation garnet shows where fibrolite has been enclosed by garnet. Scale bar is 1 mm; A) plane light; B) crossed nicols.

study using linear regression (Pigage 1976), small limits of error were shown to be essential to assess the reliability of a least-squares model. Elements occurring in small amounts commonly fall within error limits rather than providing additional constraints on the regression coefficients.

I have tried to minimize this problem by weighting each mass-balance equation according to the inverse of the variance of the mean for a particular set of analytical results (Reid *et al.* 1973). Interelement covariances were considered negligible. In this way, minor elements assumed increased importance in the regression model.

The standard weighted least-squares approach assumes that the independent variables in the regression equation are entirely free of error. This approach is valid where analyzed minerals are being modeled in terms of end-member compositions. In modeling metamorphic reactions, however, results of mineral analyses, among the independent variables, usually have errors of about the same magnitude as the dependent variable. In this situation, the problem becomes nonlinear and must be solved iteratively. Albarède & Provost (1977) have described an algorithm for solving weighted least-squares problems that recognizes errors in both the dependent and independent variables. The regression coefficients in this algorithm are calculated by minimizing the grand sum of the sums of squares of all analyzed minerals, rather than minimizing just the sums of squares of only the mineral being modeled. This algorithm was incorporated into the linear regression package PROTEUS (Fletcher & Greenwood 1979), which was used to test for possible metamorphic reactions. PROTEUS uses mineral structural formulae rather than weight percent oxides as the basis for linear regression. Oxygen has not been included in the regression calculation.

Examination of regression coefficients and residuals with this approach indicates that it gives results similar to those obtained using standard weighted linear-regression techniques. A regression model was considered significant if the modeled composition for each analyzed mineral in the regression equation was within the two-sided confidence interval calculated from the estimated standard errors for that mineral. All confidence intervals were constructed at the 95% probability level (alpha = 0.05). Appropriate *t*-factors were selected from statistical tables (Guenther 1965, p. 294).

Residuals for any regression equation will necessarily decrease as more minerals are added to the linear-regression model. Indeed, for an exact solution the residuals are zero. At the same time the two-sided confidence interval (permitted error limit) increases as more minerals are included in the model, since the number of degrees of freedom decreases. Therefore, one must be cautious in assessing the quality of a linear regression model strictly based on the size of the residuals compared to the permitted limits of error. It is also necessary to determine if the linear regression model is consistent with the chemical zoning patterns and mineral textures present in the samples.

Textural relations in pelitic units of the Shuswap complex suggest that garnet and staurolite were breaking down to form biotite–muscovite–ilmenite–fibrolitic sillimanite aggregates. The regression approach was used to model staurolite or garnet in terms of the other minerals coexisting with them. Zn was excluded from the mass-balance equations because other metamorphic studies indicate that Zn remains in relict staurolite in increasing concentrations with the progressive breakdown of matrix staurolite (Guidotti 1970, Woodsworth 1977). A fluid phase consisting of H_2O was assumed to be present. Quartz, H_2O and sillimanite were considered to be stoichiometric and free of error (Albee & Chodos 1969, Chinner *et al.* 1969, Kwak 1971a).

The regression models of staurolite and garnet should ideally use compositions of coexisting minerals at the time of initial formation of fibrolite. Based on the textural interpretation presented earlier, this would correspond to mineral compositions in equilibrium with rims of first-generation garnet. Systematic partitioning of Mg and Fe between rims of second-generation garnet and biotite (Fig. 6) indicates that the various homogeneous minerals have adjusted their compositions to remain in near-equilibrium with rim compositions of the later stage-two garnet. Consequently, compositions in equilibrium with first-generation garnet have not survived and cannot be used for the regression studies.

Though recognizing this problem, I have chosen to model staurolite and garnet breakdown using rim compositions for all minerals. Major priority, therefore, has been placed on using equilibrium compositions for coexisting minerals. The significance of this choice cannot be fully assessed. Garnet compositions differ mainly in Fe and Mn content. The biotite inclusion within garnet from sample 74, however, has a composition very similar to matrix biotite in the same sample. Regression equations must

TABLE 9. EQUATION R-1. SAMPLE 82.

REGRESSION MODEL OF STAUROLITE - GARNET INCLUDED IN MODEL.

REGRESSION COEFFICIENTS

	SILL	QRTZ	H2O	MUS	BIO	PLAG	ILM	GAR	STAU
	9.915	-1.583	2.272	-1.031	0.914	-0.044	0.095	0.248	-1.000
SIGMA	0.045	0.054	0.016	0.012	0.009	0.005	0.006	0.009	

INFORMATION PERTAINING TO THIS FIT:

RESIDUALS (X - X*)

ELEMENT	MUS	BIO	PLAG	ILM	GAR	STAU
SI+4	0.000	-0.000	0.000	0.0	-0.000	0.000
AL+3	0.000	-0.000	0.000	-0.000	-0.000	0.000
FE+2	0.009	-0.041	0.0	-0.002	-0.007	0.246
MN+2	0.0	0.001	0.0	0.000	0.003	-0.006
MG+2	-0.008	0.037	0.0	0.000	0.011	-1.288
CA+2	0.0	0.0	-0.003	0.0	0.013	-0.027
NA+1	0.196	-0.056	0.002	0.0	0.0	0.0
K+1	0.045	-0.080	0.000	0.0	0.0	0.0
H+1	0.000	-0.000	0.0	0.0	0.0	0.000
TI+4	-0.002	0.008	0.0	0.003	0.000	-0.192
BA+2	0.010	-0.000	0.0	0.0	0.0	0.0
F-1	-0.052	0.026	0.0	0.0	0.0	0.0

ERROR RATIO (RESIDUAL / PERMITTED ERROR)

ELEMENT	MUS	BIO	PLAG	ILM	GAR	STAU
SI+4	0.000	0.000	0.000	0.0	0.000	0.000
AL+3	0.000	0.000	0.000	0.000	0.000	0.000
FE+2	1.869	3.690	0.0	0.254	0.860	8.196
MN+2	0.0	1.059	0.0	0.108	1.098	2.510
MG+2	1.908	3.766	0.0	0.115	1.170	20.076
CA+2	0.0	0.0	0.768	0.0	3.824	8.751
NA+1	17.746	8.757	0.410	0.0	0.0	0.0
K+1	3.068	3.784	0.004	0.0	0.0	0.0
H+1	0.000	0.000	0.0	0.0	0.0	0.000
TI+4	0.810	1.598	0.0	0.269	0.050	7.101
BA+2	9.173	1.815	0.0	0.0	0.0	0.0
F-1	19.192	12.626	0.0	0.0	0.0	0.0

CORRELATION COEFFICIENTS

SILL	1.000							
QRTZ	-0.215	1.000						
H2O	0.454	0.425	1.000					
MUS	-0.590	-0.413	-0.638	1.000				
BIO	0.412	0.189	0.163	-0.818	1.000			
PLAG	-0.011	-0.104	-0.152	0.002	0.138	1.000		
ILM	-0.070	0.016	-0.065	0.266	-0.314	0.299	1.000	
GAR	-0.316	-0.187	-0.032	0.493	-0.664	-0.530	-0.240	1.000
	SILL	QRTZ	H2O	MUS	BIO	PLAG	ILM	GAR

be regarded as interpretive rather than strictly quantitative.

Several different possible regression models are listed in Tables 9 to 16. Equations R–1 through R–4 (Tables 9–12) use the same mineral compositions for comparative purposes (sample 82). All the models involve the breakdown of staurolite or garnet (or both) to form sillimanite. Since PROTEUS uses mineral structural formulae in the regression, the regression coefficient balances the mineral structural formula units outlined in Table 17.

Reaction R–1 (Table 9) models staurolite in terms of edge compositions of coexisting phases. Residuals are much larger than permitted error limits for several major elements. Large errors in the balancing of Mg, Fe, Na and K are especially noticeable. The large coefficients of correlation between various minerals is reflected in the large standard deviations in the regression coefficients. These large values are related to the occurrence of specific elements in only a few minerals. Errors for the muscovite coefficient, for example, are mirrored by errors in the biotite coefficient since these two minerals balance the regression equation for K.

Garnet appears as a product phase, which is in general agreement with the commonly reported staurolite-out reaction (Thompson 1976). However, this equation conflicts with observed

TABLE 10. EQUATION R-2. SAMPLE 82

REGRESSION MODEL OF STAUROLITE - ANORTHITE AND GARNET INCLUDED IN MODEL.

REGRESSION COEFFICIENTS

	SILL	ANOR	QRTZ	H2O	MUS	BIO	PLAG	ILM	GAR	STAU
	8.330	-0.206	-3.116	2.085	-0.273	0.235	0.082	0.063	1.002	-1.000
SIGMA	0.054	0.003	0.051	0.010	0.022	0.019	0.007	0.005	0.019	

INFORMATION PERTAINING TO THIS FIT:

RESIDUALS (X - X*)

ELEMENT	MUS	BIO	PLAG	ILM	GAR	STAU
SI+4	0.000	-0.000	-0.000	0.0	-0.000	0.000
AL+3	0.000	-0.000	-0.000	-0.000	-0.000	0.000
FE+2	0.000	-0.002	0.0	-0.000	-0.005	0.043
MN+2	0.0	0.001	0.0	0.000	0.040	-0.019
MG+2	-0.000	0.002	0.0	0.000	0.007	-0.205
CA+2	0.0	0.0	-0.000	0.0	-0.000	0.000
NA+1	-0.000	0.000	0.000	0.0	0.0	0.0
K+1	0.062	-0.107	-0.000	0.0	0.0	0.0
H+1	0.0	0.0	0.0	0.0	0.0	0.0
TI+4	-0.000	0.000	0.0	0.000	0.000	-0.022
BA+2	0.011	-0.000	0.0	0.0	0.0	0.0
F-1	-0.051	0.025	0.0	0.0	0.0	0.0

ERROR RATIO (RESIDUAL / PERMITTED ERROR)

ELEMENT	MUS	BIO	PLAG	ILM	GAR	STAU
SI+4	0.000	0.000	0.000	0.0	0.000	0.000
AL+3	0.000	0.000	0.000	0.000	0.000	0.000
FE+2	0.088	0.168	0.0	0.030	0.615	1.450
MN+2	0.0	0.870	0.0	0.227	14.161	8.007
MG+2	0.080	0.154	0.0	0.012	0.754	3.198
CA+2	0.0	0.0	0.000	0.0	0.000	0.000
NA+1	0.018	0.008	0.003	0.0	0.0	0.0
K+1	4.233	5.078	0.034	0.0	0.0	0.0
H+1	0.0	0.0	0.0	0.0	0.0	0.0
TI+4	0.025	0.047	0.0	0.020	0.023	0.816
BA+2	9.437	1.816	0.0	0.0	0.0	0.0
F-1	18.810	12.034	0.0	0.0	0.0	0.0

CORRELATION COEFFICIENTS

	SILL	ANOR	QRTZ	H2O	MUS	BIO	PLAG	ILM	GAR
SILL	1.000								
ANOR	0.402	1.000							
QRTZ	-0.060	0.317	1.000						
H2O	0.540	0.318	0.332	1.000					
MUS	-0.762	-0.504	-0.453	-0.699	1.000				
BIO	0.757	0.511	0.447	0.673	-0.997	1.000			
PLAG	0.720	0.411	0.408	0.674	-0.950	0.944	1.000		
ILM	-0.002	0.236	0.120	-0.059	0.092	-0.094	-0.087	1.000	
GAR	-0.744	-0.634	-0.506	-0.627	0.930	-0.933	-0.880	-0.147	1.000

garnet-breakdown textures in the Azure Lake pelites. Many of the plagioclase grains in Azure Lake pelites exhibit reverse concentric zoning (*i.e.*, rims more anorthite-rich). In equation R–2, anorthite has been included in the regression model to accommodate a changing feldspar composition during the reaction. Residuals for Na and Ca become negligible with this addition, since inclusion of anorthite allows for balancing the grossular content of the garnet. Anorthite is a reactant phase in R–2 (Table 10). This contradicts the observed compositional zoning in plagioclase.

Mg and K residuals still denote imbalances for some of the major constituents. Equation R–2 is similar to R–1, although inclusion of anorthite reduces the residuals. Garnet remains as a product phase, in contradiction to the textures described for the breakdown of stage-one garnet. Equation R–2 is consistent, however, with the growth of stage-two garnet at the expense of staurolite.

Equation R–3 (Table 11) shows that residuals for the regression are reduced significantly by the addition of rutile as a participating phase. Major element residuals are within or only slightly above permitted error limits. Mn in modeled garnet compositions is consistently lower than analyzed Mn-content. This is, at least partly, related to the difficulty in analyzing rim compositions in garnet because of the concentric zoning. Another possible explanation is that Mn-garnet is not participating in the actual reaction and is merely concentrating in

TABLE 11. EQUATION R-3. SAMPLE 82

REGRESSION MODEL OF STAUROLITE - ANORTHITE, RUTILE, AND GARNET INCLUDED IN MODEL.

REGRESSION COEFFICIENTS

	SILL	ANOR	QRTZ	H2O	RUT	MUS	BIO	PLAG	ILM	GAR	STAU
	9.262	-0.020	-1.280	2.107	-2.471	-0.345	0.297	0.103	1.280	-0.032	-1.000
SIGMA	0.043	0.004	0.055	0.009	0.054	0.015	0.012	0.005	0.027	0.019	

INFORMATION PERTAINING TO THIS FIT:

RESIDUALS (X - X*)

ELEMENT	MUS	BIO	PLAG	ILM	GAR	STAU
SI+4	-0.000	0.000	0.000	0.0	-0.000	-0.000
AL+3	-0.000	0.000	0.000	0.000	-0.000	-0.000
FE+2	-0.000	0.000	0.0	0.000	-0.000	-0.000
MN+2	0.0	0.000	0.0	0.000	-0.000	-0.000
MG+2	-0.000	0.000	0.0	0.000	-0.000	-0.000
CA+2	0.0	0.0	-0.000	0.0	0.000	0.000
NA+1	-0.000	0.000	0.000	0.0	0.0	0.0
K+1	0.061	-0.107	-0.000	0.0	0.0	0.0
H+1	-0.000	0.000	0.0	0.0	0.0	-0.000
TI+4	-0.000	0.000	0.0	0.000	-0.000	-0.000
BA+2	0.011	-0.000	0.0	0.0	0.0	0.0
F-1	-0.051	0.025	0.0	0.0	0.0	0.0

ERROR RATIO (RESIDUAL / PERMITTED ERROR)

ELEMENT	MUS	BIO	PLAG	ILM	GAR	STAU
SI+4	0.000	0.000	0.000	0.0	0.000	0.000
AL+3	0.000	0.000	0.000	0.000	0.000	0.000
FE+2	0.000	0.000	0.0	0.000	0.000	0.000
MN+2	0.0	0.000	0.0	0.000	0.000	0.000
MG+2	0.000	0.000	0.0	0.000	0.000	0.000
CA+2	0.0	0.0	0.000	0.0	0.000	0.000
NA+1	0.018	0.008	0.003	0.0	0.0	0.0
K+1	4.224	5.069	0.034	0.0	0.0	0.0
H+1	0.000	0.000	0.0	0.0	0.0	0.000
TI+4	0.000	0.000	0.0	0.000	0.000	0.000
BA+2	9.435	1.816	0.0	0.0	0.0	0.0
F-1	18.812	12.039	0.0	0.0	0.0	0.0

CORRELATION COEFFICIENTS

	SILL	ANOR	QRTZ	H2O	RUT	MUS	BIO	PLAG	ILM	GAR
SILL	1.000									
ANOR	0.215	1.000								
QRTZ	-0.286	0.565	1.000							
H2O	0.292	-0.136	0.029	1.000						
RUT	-0.140	-0.860	-0.548	0.185	1.000					
MUS	-0.470	0.212	0.026	-0.565	-0.369	1.000				
BIO	0.455	-0.204	-0.042	0.497	0.373	-0.988	1.000			
PLAG	0.394	-0.286	-0.062	0.503	0.311	-0.853	0.835	1.000		
ILM	0.124	0.876	0.555	-0.204	-0.975	0.410	-0.415	-0.346	1.000	
GAR	-0.410	-0.870	-0.602	-0.061	0.815	0.123	-0.125	-0.104	-0.818	1.000

the residual garnet. Balance is still poor for lesser constituents like Ba and F. Because these elements are present in small amounts, they could be readily balanced by small concentrations in unanalyzed phases (tourmaline or fluid phase).

Continued K imbalance may indicate increased mobility of K relative to the other elements being considered or continued adjustment of mica compositions to lower temperatures during cooling. Alternatively, this imbalance may be an algebraic consequence of the assumption that the system is isochemical with respect to Ba and F. If these two elements are considered to be mobile and therefore deleted from the regression equation, then the algebraic decrease in the number of elements would result in an exact algebraic solution for the breakdown of staurolite in sample 82. This exact solution is presented in equation R–4 (Table 12).

Including rutile in equations R–3 and R–4 has caused garnet to appear as a reactant phase. This is consistent with the textural interpretation for the breakdown of stage-one garnet. Anorthite is a reactant phase but participates in the suggested reaction only to a minor extent; this may be partly an algebraic result of using the more calcic composition of the rim in the linear regression model.

The considerable improvement in residuals for equation R–3 suggests that rutile must be included as a participating reactant phase in the initial formation of fibrolite aggregates. This is also supported by the correspondence between the regression equation and the observed textures. Problems with balancing of minor elements may be related to unanalyzed phases or to increased mobility of these elements. The regression equations are dehydration reactions and are consistent with an overall increasing meta-

TABLE 12. EQUATION R-4. SAMPLE 82.

ALGEBRAIC SOLUTION MODEL OF STAUROLITE - GARNET, ANORTHITE, AND RUTILE INCLUDED IN MODEL.

REACTION COEFFICIENTS

SILL	ANOR	QRTZ	H2O	RUT	GAR	MUS	BIO	PLAG	ILM	STAU
9.170	-0.016	-1.364	2.040	-2.474	-0.032	-0.308	0.295	0.088	1.281	-1.000

INFORMATION PERTAINING TO THIS FIT:

RESIDUALS AND ERROR RATIOS ARE ALL 0.0 FOR THIS MODEL.

CORRELATION COEFFICIENTS

	SILL	ANOR	QRTZ	H2O	RUT	GAR	MUS	BIO	PLAG	ILM
SILL	1.000									
ANOR	0.263	1.000								
QRTZ	-0.317	0.576	1.000							
H2O	0.157	-0.072	0.033	1.000						
RUT	-0.181	-0.854	-0.570	0.079	1.000					
GAR	-0.415	-0.887	-0.592	-0.026	0.816	1.000				
MUS	-0.398	0.169	0.087	-0.299	-0.366	0.123	1.000			
BIO	0.380	-0.160	-0.106	0.212	0.372	-0.125	-0.986	1.000		
PLAG	0.327	-0.244	-0.109	0.284	0.302	-0.102	-0.838	0.815	1.000	
ILM	0.169	0.867	0.580	-0.085	-0.975	-0.818	0.408	-0.415	-0.337	1.000
	SILL	ANOR	QRTZ	H2O	RUT	GAR	MUS	BIO	PLAG	ILM

morphic grade toward the southwest.

Rutile occurs only as scattered inclusions in porphyroblastic kyanite and garnet in the Azure Lake schists. Lack of rutile in the schist matrix suggests that reaction textures are partly preserved because of the exhaustion of available rutile.

Equation R–2 contains garnet as a product phase. This equation reasonably describes the formation of stage-two garnet concomitantly with continued growth of biotite and fibrolite. Problems concerning the imbalance of major and minor elements have already been discussed.

Reactions R–5 through R–8 (Tables 13–16) show that similar reaction relations are revealed when regression models are calculated for other samples containing staurolite or garnet (or both) with sillimanite. Reaction equations R–5 and R–6 show reaction relations for sample 2–376. Staurolite and rutile are not present in the mode and, therefore, were not included in the initial regression calculations. Garnet-rim compositions for this sample were modeled in terms of the other coexisting minerals.

Equation R–5 contains extremely large errors in K and Mg with lesser but significant errors in Mn, Ba, and F. In equation R–6, rutile has been included as a participating phase. Residuals for Mg and K are reduced significantly. Major element residuals are within permitted error limits or only slightly exceed these limits. Ba and F remain poorly balanced in the regression calculations. Exclusion of these two minor elements from the regression equation does not appreciably alter the regression coefficients. Mn continues to have slightly large residuals.

Equations R–5 and R–6 delineate the breakdown of garnet to form fibrolite–biotite–ilmenite aggregates. As with sample 82, inclusion of rutile as a reactant phase significantly improves the regression modeling. The absence of rutile in the mode suggests that reaction textures were preserved at least partly because of exhaustion of matrix rutile. In each of these equations, muscovite occurs as a reactant phase; this contradicts the observed textural relations and will be discussed in a later section.

Equation R–7 models staurolite in terms of coexisting phases for sample 223. Both rutile and anorthite have been included in the regression equation. Error ratios indicate that residuals are small for all major elements. Error problems with Ba and F also do not appear to be major in this model. The occurrence of the different participating phases as reactants or products is generally consistent with mineral textures.

Equation R–8 presents the regression model for sample 40. Rutile is not present in the mode and was excluded from the regression. All residuals except Mn, Ba, and F are within the permitted error limits. The overall fit in the equation is quite reasonable. Sample 40 contains only stage-two garnet; first-generation garnet is no longer present. Textural studies have indicated that stage-two garnet is a product of a prograde metamorphic reaction forming after the initial formation of the fibrolite aggregates. Equation R–8 is consistent with this interpretation, since garnet occurs as a product phase in the equation. This equation indicates that sillimanite and biotite continue to form concomitantly with the growth of stage-two garnet. Rutile, in this instance, does not dramatically improve the residuals and probably does

TABLE 13. EQUATION R-5. SAMPLE 2-376.

REGRESSION MODEL OF GARNET - ANORTHITE INCLUDED IN MODEL.

REGRESSION COEFFICIENTS

	SILL	ANOR	QRTZ	H2O	MUS	BIO	PLAG	ILM	GAR
	14.155	-0.397	12.357	9.199	-5.772	1.187	2.225	0.108	-1.000
SIGMA	0.209	0.010	0.194	0.153	0.081	0.006	0.033	0.004	

INFORMATION PERTAINING TO THIS FIT:

RESIDUALS (X - X*)

ELEMENT	MUS	BIO	PLAG	ILM	GAR
SI+4	0.000	-0.000	0.0	0.0	0.000
AL+3	0.000	-0.000	0.0	-0.000	0.000
FE+2	0.008	-0.020	0.0	-0.017	0.008
MN+2	0.0	-0.007	0.0	-0.007	0.039
MG+2	-0.209	0.222	0.0	0.000	-0.051
CA+2	0.0	-0.000	0.0	-0.000	0.000
NA+1	-0.000	0.000	0.0	0.0	0.0
K+1	1.182	-0.314	0.0	0.0	0.0
H+1	0.000	-0.000	0.0	0.0	0.0
TI+4	-0.011	0.012	0.0	0.014	-0.000
BA+2	0.011	-0.000	0.0	0.0	0.0
F-1	-0.008	0.009	0.0	0.0	0.0

ERROR RATIO (RESIDUAL / PERMITTED ERROR)

ELEMENT	MUS	BIO	PLAG	ILM	GAR
SI+4	0.000	0.000	0.0	0.0	0.000
AL+3	0.000	0.000	0.0	0.000	0.000
FE+2	3.695	2.576	0.0	0.627	1.454
MN+2	0.0	12.747	0.0	3.454	27.009
MG+2	51.161	23.768	0.0	0.097	10.059
CA+2	0.0	0.000	0.0	0.000	0.000
NA+1	0.111	0.026	0.0	0.0	0.0
K+1	112.777	26.203	0.0	0.0	0.0
H+1	0.000	0.000	0.0	0.0	0.0
TI+4	5.547	2.578	0.0	0.732	0.218
BA+2	20.778	1.936	0.0	0.0	0.0
F-1	9.304	4.325	0.0	0.0	0.0

CORRELATION COEFFICIENTS

	SILL	ANOR	QRTZ	H2O	MUS	BIO	PLAG	ILM
SILL	1.000							
ANOR	-0.917	1.000						
QRTZ	0.967	-0.892	1.000					
H2O	0.994	-0.915	0.978	1.000				
MUS	-0.995	0.917	-0.977	-0.997	1.000			
BIO	0.714	-0.670	0.671	0.702	-0.741	1.000		
PLAG	0.974	-0.936	0.947	0.978	-0.980	0.716	1.000	
ILM	0.472	-0.424	0.490	0.485	-0.453	-0.743	0.453	1.000

not constitute a participating phase in the prograde reaction.

Interpretation

The zoning and inclusion patterns in garnet crystals imply two periods of growth, with the second occurring after initial formation of fibrolite aggregates. Both first- and second-stage growth resulted from a continuous garnet-forming reaction during prograde metamorphism. Any growth-zoning patterns in stage-one garnet have been destroyed by homogenization through diffusion. The hiatus between first- and second-generation garnets may be explained by resorption of garnet through a discontinuous garnet-breakdown reaction to form sillimanite.

Sillimanite-forming reactions have been modeled for Azure Lake mineral compositions using linear regression techniques. Regression modeling of garnet- and staurolite-breakdown reactions indicates that rutile is required as a reactant phase in the sillimanite-forming reactions involving the breakdown of stage-one garnet. Reaction textures in the schists are partly preserved because of exhaustion of matrix rutile. Prograde growth of second-stage garnet has also been modeled using linear regression.

TABLE 14. EQUATION R-6. SAMPLE 2-376.

REGRESSION MODEL OF GARNET - ANORTHITE AND RUTILE INCLUDED IN MODEL.

REGRESSION COEFFICIENTS

	SILL	ANOR	QRTZ	H2O	RUT	MUS	BIO	PLAG	ILM	GAR
	1.003	0.197	1.746	0.063	-2.137	-0.199	0.172	0.061	1.053	-1.000
SIGMA	0.007	0.003	0.007	0.002	0.016	0.002	0.001	0.001	0.007	

INFORMATION PERTAINING TO THIS FIT:

RESIDUALS (X - X*)

ELEMENT	MUS	BIO	PLAG	ILM	GAR
SI+4	0.000	-0.000	-0.000	0.0	0.000
AL+3	0.000	-0.000	-0.000	-0.000	0.000
FE+2	-0.000	0.001	0.0	0.077	-0.004
MN+2	0.0	-0.000	0.0	-0.023	0.014
MG+2	0.000	-0.002	0.0	-0.000	0.003
CA+2	0.0	-0.000	-0.000	-0.000	0.000
NA+1	-0.000	0.000	0.000	0.0	0.0
K+1	0.058	-0.065	-0.000	0.0	0.0
H+1	0.0	0.0	0.0	0.0	0.0
TI+4	-0.000	0.000	0.0	0.000	-0.000
BA+2	0.006	-0.001	0.0	0.0	0.0
F-1	-0.020	0.088	0.0	0.0	0.0

ERROR RATIO (RESIDUAL / PERMITTED ERROR)

ELEMENT	MUS	BIO	PLAG	ILM	GAR
SI+4	0.000	0.000	0.000	0.0	0.000
AL+3	0.000	0.000	0.000	0.000	0.000
FE+2	0.060	0.177	0.0	2.906	0.690
MN+2	0.0	0.642	0.0	11.732	9.395
MG+2	0.111	0.218	0.0	0.060	0.637
CA+2	0.0	0.000	0.000	0.000	0.000
NA+1	0.005	0.005	0.005	0.0	0.0
K+1	5.579	5.453	0.055	0.0	0.0
H+1	0.0	0.0	0.0	0.0	0.0
TI+4	0.000	0.000	0.0	0.000	0.000
BA+2	11.152	4.372	0.0	0.0	0.0
F-1	22.667	44.324	0.0	0.0	0.0

CORRELATION COEFFICIENTS

	SILL	ANOR	QRTZ	H2O	RUT	MUS	BIO	PLAG	ILM
SILL	1.000								
ANOR	-0.535	1.000							
QRTZ	-0.086	-0.475	1.000						
H2O	0.459	-0.041	0.318	1.000					
RUT	0.049	-0.005	-0.018	0.039	1.000				
MUS	-0.461	0.049	-0.141	-0.755	-0.134	1.000			
BIO	0.280	-0.037	-0.074	0.260	0.166	-0.822	1.000		
PLAG	0.399	-0.058	0.108	0.710	0.102	-0.845	0.629	1.000	
ILM	-0.059	0.006	0.024	-0.045	-0.851	0.166	-0.209	-0.126	1.000

The regression equations indicate that growth of second-stage garnet is concurrent with continued formation of sillimanite–biotite–ilmenite aggregates. Rutile does not appear to be a participating phase in this sillimanite-forming reaction.

The regression equations have generally verified the simplified metamorphic reactions presented for the KFMASH system (see above). Use of the linear regression approach has allowed for incorporation of additional components not considered in the simplified system. The generally small residuals in the regression equations substantiate the initial assumption that the sillimanite-forming reactions are essentially isochemical.

Muscovite is required as a reactant in all of the above regression equations. Textures, however, indicate that coarse, equant muscovite is a product phase within the fibrolite aggregates and that it replaces kyanite and staurolite. Carmichael (1969) has suggested that textural relations between minerals are controlled by local cation-exchange reactions (ionic reactions). The "general" metamorphic reaction results from the summation of two or more different local reactions. The local reactions are coupled by ionic diffusion, so that the system is closed to mass transfer on the scale of a thin section. His example of the local replacement of kyanite by muscovite, concomitant with the formation of sillimanite in nearby muscovite grains, is directly applicable to schists from the Azure Lake area. In this case, an overall decrease in modal muscovite due to staurolite or garnet

TABLE 15. EQUATION R-7. SAMPLE 223.

REGRESSION MODEL OF STAUROLITE - GARNET, ANORTHITE, AND RUTILE INCLUDED IN MODEL.

REGRESSION COEFFICIENTS

	SILL	ANOR	QRTZ	H2O	RUT	GAR	MUS	BIO	PLAG	ILM	STAU
	9.110	-0.029	-1.370	2.029	-2.504	-0.014	-0.292	0.285	0.092	1.308	-1.000
SIGMA	0.011	0.001	0.020	0.003	0.016	0.006	0.004	0.004	0.003	0.008	

INFORMATION PERTAINING TO THIS FIT:

RESIDUALS (X - X*)

ELEMENT	GAR	MUS	BIO	PLAG	ILM	STAU
SI+4	0.000	0.000	-0.000	0.0	0.0	0.000
AL+3	0.000	0.000	-0.000	0.0	0.0	0.000
FE+2	0.000	0.000	-0.000	0.0	0.0	0.000
MN+2	0.000	0.0	0.000	0.0	0.0	-0.000
MG+2	0.000	0.002	-0.006	0.0	0.0	0.030
CA+2	0.000	0.000	-0.000	0.0	0.0	0.0
NA+1	0.0	-0.000	0.000	0.0	0.0	0.0
K+1	0.0	-0.000	0.000	0.0	0.0	0.0
H+1	0.0	0.000	-0.000	0.0	0.0	0.000
TI+4	0.0	-0.000	0.000	0.0	0.0	-0.000
BA+2	0.0	0.003	-0.001	0.0	0.0	0.0
F-1	0.0	-0.004	0.005	0.0	0.0	-0.025

ERROR RATIO (RESIDUAL / PERMITTED ERROR)

ELEMENT	GAR	MUS	BIO	PLAG	ILM	STAU
SI+4	0.000	0.000	0.000	0.0	0.0	0.000
AL+3	0.000	0.000	0.000	0.0	0.0	0.000
FE+2	0.000	0.001	0.007	0.0	0.0	0.020
MN+2	0.015	0.0	0.061	0.0	0.0	0.373
MG+2	0.003	0.234	0.402	0.0	0.0	1.629
CA+2	0.000	0.000	0.000	0.0	0.0	0.0
NA+1	0.0	0.016	0.003	0.0	0.0	0.0
K+1	0.0	0.031	0.012	0.0	0.0	0.0
H+1	0.0	0.000	0.000	0.0	0.0	0.000
TI+4	0.0	0.000	0.000	0.0	0.0	0.000
BA+2	0.0	3.043	1.395	0.0	0.0	0.0
F-1	0.0	1.388	1.591	0.0	0.0	6.458

CORRELATION COEFFICIENTS

	SILL	ANOR	QRTZ	H2O	RUT	GAR	MUS	BIO	PLAG	ILM
SILL	1.000									
ANOR	0.239	1.000								
QRTZ	-0.126	0.504	1.000							
H2O	0.227	-0.107	0.062	1.000						
RUT	-0.168	-0.760	-0.467	0.069	1.000					
GAR	-0.450	-0.761	-0.483	-0.018	0.798	1.000				
MUS	-0.467	0.231	0.072	-0.321	-0.405	0.110	1.000			
BIO	0.423	-2.11	-0.104	0.170	0.418	-0.114	-0.972	1.000		
PLAG	0.185	-0.595	-0.190	0.194	0.199	-0.054	-5.042	0.478	1.000	
ILM	0.153	0.758	0.466	-0.072	-0.996	-0.785	0.432	-0.446	-0.212	1.000
	SILL	ANOR	QRTZ	H2O	RUT	GAR	MUS	BIO	PLAG	ILM

breakdown may be accompanied by the local formation of coarse muscovite around kyanite. Similar ionic reactions would account for the replacement of other phases by muscovite.

Alternatively, coarse muscovite may result from a change in metamorphic conditions at some indeterminate time after the formation of the fibrolite aggregates. Eugster (1970) and Kwak (1971b) have shown that ionic reactions relating muscovite and the aluminosilicate polymorphs are very sensitive to slight changes in concentrations of ionic species (K^+ and H^+) dissolved in the fluid phase. A small change in fluid composition during metamorphism would cause muscovite to locally replace kyanite or sillimanite. Any such muscovite-forming reaction could not simply be retrograding according to the probable reactions outlined by the regression equations, since newly formed rutile was not observed. Observed textures substantiate the later replacement of other metamorphic minerals by coarse muscovite, indicating that at least part of the muscovite textures may be related to this model.

Fletcher & Greenwood (1979) have discussed identical metamorphic textures in schists from the Shuswap complex just northwest of the Azure Lake area. They argued that two metamorphic episodes are required to explain the observed textural and zoning patterns. In their suggested sequence of reactions, sillimanite is the last metamorphic mineral to crystallize. In contrast, I have attempted to show that these textures may be explained by a sequence of reactions during a single episode of prograde metamorphism. With this interpretation the initial formation of fibrolite aggregates preceded growth of the second generation of garnet. Muscovite textures may be partly related to changes in fluid compositions during late stages of the same metamorphic event.

TABLE 16. EQUATION R-8. SAMPLE 40.

REGRESSION MODEL OF STAUROLITE - GARNET AND ANORTHITE INCLUDED IN MODEL.

REGRESSION COEFFICIENTS

	SILL	ANOR	QRTZ	H2O	GAR	MUS	BIO	PLAG	ILM	STAU
	8.020	-0.169	-3.464	2.010	1.128	-0.103	0.099	0.033	0.047	-1.000
SIGMA	0.015	0.003	0.018	0.002	0.005	0.003	0.003	0.001	0.001	

INFORMATION PERTAINING TO THIS FIT:

RESIDUALS (X - X*)

ELEMENT	GAR	MUS	BIO	PLAG	ILM	STAU
SI+4	-0.000	0.000	-0.000	-0.000	0.0	0.000
AL+3	0.0	0.0	0.0	0.0	0.0	0.0
FE+2	-0.000	0.000	-0.000	0.0	-0.000	0.001
MN+2	0.062	0.0	0.000	0.0	0.000	-0.001
MG+2	-0.000	0.000	-0.001	0.0	-0.000	0.001
CA+2	0.000	0.0	0.0	0.000	0.0	0.0
NA+1	0.0	-0.000	0.000	0.000	0.0	0.0
K+1	0.0	-0.001	0.004	0.000	0.0	0.0
H+1	0.0	0.0	0.0	0.0	0.0	0.0
TI+4	-0.000	0.000	-0.000	0.0	-0.000	0.000
BA+2	0.0	0.001	-0.005	-0.000	0.0	0.0
F-1	0.0	-0.000	0.002	0.0	0.0	-0.003

ERROR RATIO (RESIDUAL / PERMITTED ERROR)

ELEMENT	GAR	MUS	BIO	PLAG	ILM	STAU
SI+4	0.000	0.000	0.000	0.000	0.0	0.000
AL+3	0.0	0.0	0.0	0.0	0.0	0.0
FE+2	0.016	0.001	0.004	0.0	0.001	0.043
MN+2	8.167	0.0	0.057	0.0	0.016	1.106
MG+2	0.032	0.002	0.028	0.0	0.002	0.107
CA+2	0.000	0.0	0.0	0.000	0.0	0.0
NA+1	0.0	0.004	0.004	0.000	0.0	0.0
K+1	0.0	0.197	0.317	0.003	0.0	0.0
H+1	0.0	0.0	0.0	0.0	0.0	0.0
TI+4	0.001	0.001	0.001	0.0	0.001	0.009
BA+2	0.0	1.482	3.966	0.076	0.0	0.0
F-1	0.0	0.066	0.213	0.0	0.0	0.913

CORRELATION COEFFICIENTS

	SILL	ANOR	QRTZ	H2O	GAR	MUS	BIO	PLAG	ILM
SILL	1.000								
ANOR	-0.104	1.000							
QRTZ	-0.407	-0.055	1.000						
H2O	0.105	0.012	0.066	1.000					
GAR	-0.431	-0.210	-0.444	-0.124	1.000				
MUS	-0.398	-0.098	-0.234	-0.252	0.658	1.000			
BIO	0.392	0.102	0.228	0.189	-0.667	-0.987	1.000		
PLAG	0.336	0.061	0.174	0.238	-0.558	-0.858	0.838	1.000	
ILM	-0.005	0.024	0.049	-0.018	-0.060	0.125	-0.129	-0.105	1.000

TABLE 17. MINERAL FORMULAE USED IN PROTEUS

MINERAL	NUMBER OF O,OH,F
GARNET	12
MUSCOVITE	24
BIOTITE	24
STAUROLITE	48
PLAGIOCLASE	8
K-FELDSPAR	8
ILMENITE	6
QUARTZ	2
RUTILE	2
ANORTHITE	8
SILLIMANITE	5

Acknowledgements

This paper represents part of a Ph.D. thesis completed at the University of British Columbia. Discussions with H.J. Greenwood concerning linear regression techniques have contributed extensively to this study. Reviews by F.S. Spear and J.H. Stout helped isolate problem areas in the original manuscript. Field and laboratory expenses were defrayed through research grant NRCC 67-4222 to H.J. Greenwood. I was supported by research fellowships from the National Science Foundation (NSF) and the In-

TABLE 18. ANALYSES FOR SAMPLE 82

MINERAL ANALYSES	GAR 23	MUS 13	BIO 11	STAU 6	PLAG 23	ILM 6
SIO2	37.74(0.05)#	46.85(0.08)	36.81(0.08)	27.40(0.09)	61.60(0.07)	NA
TIO2	0.01(0.004)	0.69(0.01)	2.18(0.02)	0.68(0.05)	NA	52.76(0.11)
AL2O3	21.49(0.03)	36.20(0.06)	19.50(0.06)	53.67(0.21)	23.98(0.04)	0.06(0.008)
FEO*	36.22(0.06)	1.21(0.02)	19.00(0.04)	13.30(0.05)	NA	46.67(0.09)
ZNO	NA	NA	NA	1.18(0.03)	NA	0.04(0.007)
MNO	1.04(0.02)	-	0.01(0.003)	0.05(0.004)	NA	0.25(0.01)
MGO	2.81(0.02)	0.71(0.01)	9.80(0.02)	1.43(0.06)	NA	0.07(0.02)
CAO	2.18(0.02)	-	-	0.01(0.004)	5.94(0.04)	-
BAO	NA	0.41(0.01)	0.20(0.002)	NA	-	NA
NA2O	NA	1.21(0.02)	0.36(0.01)	NA	8.46(0.03)	NA
K2O	NA	9.42(0.04)	8.65(0.05)	NA	0.07(0.003)	NA
F	NA	0.06(0.003)	0.24(0.002)	-	NA	NA
H2O$	NA	4.55(0.005)	3.92(0.005)	2.15(0.007)	NA	NA
SUBTOTAL		101.31	100.67	99.87		
LESS O=F		0.03	0.10	-		
TOTAL	101.49	101.28	100.57	99.87	100.05	99.85

NA = NOT ANALYZED
# ESTIMATED STANDARD ERRORS ENCLOSED IN PARENTHESES
* TOTAL IRON AS FEO
$ H2O CALCULATED FROM STRUCTURAL FORMULA.
STANDARD ERROR FOR H2O CALCULATED FROM STANDARD ERRORS OF OTHER ELEMENTS USING MONTE CARLO APPROACH.

ternational Nickel Company (INCO). The manuscript was typed and retyped by L. Taylor and M. Watkins.

References

ALBARÈDE, F. & PROVOST, A. (1977): Petrological and geochemical mass-balance equations: an algorithm for least-square fitting and general error analysis. *Computers Geosci.* **3**, 309-326.

ALBEE, A.L. & CHODOS, A.A. (1969): Minor element content of coexistent Al_2SiO_5 polymorphs. *Amer. J. Sci.* **267**, 310-316.

ANDERSON, D.E. & OLIMPIO, J.C. (1977): Progressive homogenization of metamorphic garnets, South Morar, Scotland: evidence for volume diffusion. *Can. Mineral.* **15**, 205-216.

ANDERSON, G.M. (1976): Error propagation by the Monte Carlo method in geochemical calculations. *Geochim. Cosmochim. Acta* **40**, 1533-1538.

BEVINGTON, P.R. (1969): *Data Reduction and Error Analysis for the Physical Sciences.* McGraw-Hill, New York.

CAMPBELL, R.B. (1968): Canoe River, British Columbia. *Geol. Surv. Can. Map* **15-1967.**

——— (1977): The Shuswap metamorphic complex, British Columbia. *Geol. Soc. Amer. Abstr. Program* **9**, 920.

CARMICHAEL, D.M. (1969): On the mechanism of prograde metamorphic reactions in quartz-bearing pelitic rocks. *Contr. Mineral. Petrology* **20**, 244-267.

——— (1970): Intersecting isograds in the Whetstone Lake area, Ontario. *J. Petrology* **11**, 147-181.

CHAKRABORTY, K.R. & SEN, S.K. (1967): Regional metamorphism around Kandra, Singhbhum, Bihar. *Contr. Mineral. Petrology* **16**, 210-232.

CHINNER, G.A., SMITH, J.V. & KNOWLES, C.R. (1969): Transition metal contents of Al_2SiO_5 polymorphs. *Amer. J. Sci.* **267A**, 96-113.

EUGSTER, H.P. (1970): Thermal and ionic equilibria among muscovite, K-feldspar, and aluminosilicate assemblages. *Fortschr. Mineral.* **47**, 106-123.

EVANS, B.W. & GUIDOTTI, C.V. (1966): The sillimanite–potash feldspar isograd in western Maine, U.S.A. *Contr. Mineral. Petrology* **12**, 25-62.

FLETCHER, C.J.N. & GREENWOOD, H.J. (1979): Metamorphism and structure of Penfold Creek area, near Quesnel Lake, British Columbia. *J. Petrology* **20**, 743-794.

GRAY, N.H. (1973): Estimation of parameters in petrologic materials balance equations. *J. Math. Geol.* **5**, 225-236.

GREENWOOD, H.J. (1968): Matrix methods and the phase rule in petrology. *Int. Geol. Congr. 23rd (Prague)* **6**, 267-279.

——— (1975): Thermodynamically valid projections of extensive phase relationships. *Amer. Mineral.* **60**, 1-8.

GUENTHER, W.C. (1965): *Concepts of Statistical Reference.* McGraw-Hill, New York.

GUIDOTTI, C.V. (1970): The mineralogy and petrology of the transition from the lower to upper sillimanite zone in the Oquossoc area, Maine. *J. Petrology* **11**, 277-336.

———, HERD, H.H. & TUTTLE, C.L. (1973): Composition and structural state of K-feldspars from K-feldspar + sillimanite grade rocks in northwestern Maine. *Amer. Mineral.* **58**, 705-716.

HARTE, B. & HENLEY, K.J. (1966): Occurrence of compositionally zoned almanditic garnets in regionally metamorphosed rocks. *Nature* **210**, 689-692.

HOLLISTER, L.S. (1966): Garnet zoning: an interpretation based on the Rayleigh fractionation model. *Science* **154**, 1647-1651.

KWAK, T.A.P. (1971a): Compositions of natural sillimanites from volcanic inclusions and metamorphic rocks. *Amer. Mineral.* **56**, 1750-1759.

——— (1971b): The selective replacement of the aluminum silicates by white mica. *Contr. Mineral. Petrology* **32**, 193-210.

LUNDGREN, L.W. (1966): Muscovite reactions and partial melting in southeastern Connecticut. *J. Petrology* **7**, 421-453.

MARK, D.M. & CHURCH, M. (1977): On the misuse of regression in earth science. *Math. Geol.* **9**, 63-75.

PIGAGE, L.C. (1976): Metamorphism of the Settler schist, southwest of Yale, British Columbia. *Can. J. Earth Sci.* **13**, 405-421.

——— (1977): Rb–Sr dates for granodiorite intrusions on the northeast margin of the Shuswap metamorphic complex, Cariboo Mountains, British Columbia. *Can. J. Earth Sci.* **14**, 1690-1695.

——— (1978): *Metamorphism and Deformation on the Northeast Margin of the Shuswap Metamorphic Complex, Azure Lake, British Columbia.* Ph.D. thesis, Univ. British Columbia, Vancouver, B.C.

——— & GREENWOOD, H.J. (1982): Internally consistent estimates of pressure and temperature: the staurolite problem. *Amer. J. Sci.* **282**, 943-969.

REID, M.J., GANCARZ, A.J. & ALBEE, A.L. (1973): Constrained least-squares analysis of petrologic problems with an application to lunar sample 12040. *Earth Planet. Sci. Lett.* **17**, 433-445.

RUCKLIDGE, J. & GASPARRINI, E. (1969): EMPADR VII. Specifications of a computer program for processing electron microprobe analytical data. *Dep. Geology, Univ. Toronto.*

SUTHERLAND, BROWN, A. (1963): Geology of the Cariboo River area, British Columbia. *B. C. Dep. Mines Petrol. Resour. Bull.* **47**.

THOMPSON, A.B. (1976): Mineral reactions in pelitic rocks. I. Prediction of P–T–*X*(Fe–Mg) phase relations. *Amer. J. Sci.* **276**, 401-424.

———, TRACY, R.J., LYTTLE, P.T. & THOMPSON, J.B., JR. (1977): Prograde reaction histories deduced from compositional zonation and mineral inclusions in garnet from the Gassetts schist, Vermont. *Amer. J. Sci.* **277**, 1152-1167.

THOMPSON, J.B., JR. (1957): The graphical analysis of mineral assemblages in pelitic schists. *Amer. Mineral.* **42**, 842-858.

TRACY, R.J. (1978): High grade metamorphic reactions and partial melting in pelitic schist, west-central Massachusetts. *Amer. J. Sci.* **278**, 150-178.

———, ROBINSON, P. & THOMPSON, A.B. (1976): Garnet composition and zoning in the determination of temperature and pressure of metamorphism, central Massachusetts. *Amer. Mineral.* **61**, 762-775.

TRZCIENSKI, W.E., JR. (1977): Garnet zoning – product of a continuous reaction. *Can. Mineral.* **15**, 250-256.

WHEELER, J.O. & GABRIELSE, H. (1972): The Cordilleran structural province. *In* Variations in Tectonic Styles in Canada (R.A. Price & R.J.W. Douglas, eds.). *Geol. Assoc. Can. Spec. Pap.* **11**, 1-81.

WOODSWORTH, G.J. (1977): Homogenization of zoned garnets from pelitic schists. *Can. Mineral.* **15**, 230-242.

YARDLEY, B.W.D. (1977): The nature and significance of the mechanism of sillimanite growth in the Connemara schists, Ireland. *Contr. Mineral. Petrology* **65**, 53-58.

Received May 1981, revised manuscript accepted February 1982.